Microclimate Risks and Consumer Adaptation*

Jianwei Xing

Kangkai Wang

Hua Zhang

Shuang Zhang

Eric Zou

[Preliminary. Please don't share.]

July 2025

Abstract

This paper studies the economic consequences of microclimate variation—neighborhood-level temperature differences—using data from a large city in China. We combine localized temperature measures with payment records from 150,000 restaurants to estimate how localized heat affects business outcomes. We show that higher local temperatures reduce restaurant revenue and consumer foot traffic, even conditional on citywide temperature variability. Green infrastructure—parks, trees, waterways—attenuates these effects. We estimate a discrete choice model of consumer behavior and show that consumers adapt, shifting their activity toward cooler, greener, and bluer areas on hot days. This adaptation explains a substantial share of the business impacts we observe. We use our structural estimates to value urban microclimate amenities, finding that the study city's investments in urban forests and wetlands yield substantial returns in the form of improved consumer welfare and resilience to climate stress. These results demonstrate the sizable economic gains from micro-scale adaptation and highlight location microclimate management as an important part of business strategies in the face of rising climate risks.

Keywords: Microclimate; urban heat island; consumer adaptation; business climate resilience

JEL Codes: D12, L83, Q51, Q54, R11

---

* Xing: China Center for Economic Research, National School of Development, Peking University (email: jerryxing@nsd.pku.edu.cn); Wang: Guanghua School of Management, Peking University (email: kkwangecon@stu.pku.edu.cn); Zhang: China-Europe International Business School (email: zhua@ceibs.edu); Zhang: Imperial College London and CEPR (email: s.zhang@imperial.ac.uk); Zou: Ross School of Business, University of Michigan and NBER (email: ericzou@umich.edu). Xing acknowledges the support of the National Science Foundation of China (Grant Number 72303007). All errors are our own.

1. Introduction

Climate conditions can vary significantly within a city, shaped by the distribution of urban economic activities and ecological features. These interactions give rise to sharp differences in air temperature, pollution levels, and other environmental amenities, even between neighborhoods separated by only a few blocks. As cities face growing climate stress, much remains unknown about the economic significance of these hyper-local environmental variations and the extent to which adaptation occurs. This paper uses unique data to provide new estimates of how within-city climate variation—which we will refer to as *microclimate*—shapes economic behavior.

Our study focuses on Guangzhou, China's fourth-largest city with a population of 15 million. The southern Chinese metropolis faces a challenging thermal environment, with average summer daily temperatures around 28.5°C. At the same time, Guangzhou is distinguished by its rich ecological features, sitting on the coast of the Pearl River Delta and characterized by extensive urban forestry resources—the result of decades of deliberate ecological management. In addition, the service sector in Guangzhou accounts for more than 70% of GDP, much higher than the national average. Service economies tend to be more urbanized and infrastructure-dependent, and can be disrupted by climate event more immediately, compared to heavier industries that can absorb shocks over longer periods. This unique combination of dense urbanization, tertiarization and abundant green and water resources makes Guangzhou an ideal setting to examine how microclimate variability affects economic behavior and adaptation strategies.

We begin by characterizing *microclimate risks* – the degree to which hyper localized temperature variability matters for economic activities. We merge two sets of data. The first is a remote-sensing-based measurement of land surface temperature at a 1 km spatial resolution, which gives us a state-of-the-art assessment of microclimate conditions. The second is a unique administrative database of detailed records of restaurant consumption across more than 150,000 dining establishments citywide. We use this merged dataset to estimate the reduced-form relationship between restaurant performance—measured by consumer traffic and revenue—and local temperature variability in the immediate vicinity of each establishment. Our approach builds on the standard climate impact estimation framework, commonly used to study the effects of weather shocks on health and productivity. However, unlike prior studies, we apply this

framework at a hyper-local scale, isolating the effects of *micro* temperature variability near restaurant establishments from the broader, city-level *macro* temperature conditions—or what we typically consider as "today's temperature."

Our findings reveal a significant microclimate effect. Compared to a comfortable day in the 20°C-ish range, each day where a restaurant's micro temperature exceeds 30°C leads to an approximate 10% reduction in weekly business volume and revenue. Notably, only a small portion of this effect can be attributed to supply-side factors. For example, while we observe more store closures during extreme heat, these supply contractions are insufficient to explain the majority of the observed decline in performance. Instead, microclimate risks appear to be primarily driven by changes in consumer demand.

The second part of the paper analyzes consumer adaptation to microclimate risks. For decades, the city government has invested in ecological management, including expanding urban green spaces, preserving wetland areas on the city's outskirts, and creating artificial water bodies. We demonstrate that these intuitive measures have indeed served as effective adaptive strategies against microclimate risks, where proximity to urban green spaces and waterways is associated with significant reduction in micro temperature.

Do consumers value these microclimate adaptive features, and more broadly, do consumer choices respond to microclimate shocks? Our restaurant transaction data allow us to track individual consumers, observe where they choose to dine, identify their choice set, and measure the price and microclimate features of their options. Leveraging these rich data, we develop an empirical framework to estimate consumer adaptation.

We first write down a discrete choice model in which a consumer selects a dining option from a set of candidate restaurants based on trade-offs across three key dimensions: travel cost, food prices, and environmental amenities at each restaurant. Travel is likely a salient component in consumer choice in our context. In the data, most consumers exhibit a strong preference for a few dining hubs – geographical clusters of dining choices that appear to be their habitual bases. We treat the primary dining hub as a default or home base for dining choices and define travel cost as the distance a consumer must travel to deviate from this hub. We measure price as the average amount paid by all consumers dining at a given restaurant on a specific day, which reflects daily fluctuations in supply and changes in the competitive environment. We also observe

competitor restaurants' prices and operating hours, which we use as price instruments. Environmental amenities include the restaurant's micro temperature and the presence of green spaces and water bodies nearby. We also consider air quality and precipitation, which are important components of microclimate and could conceivably be important for dining choices as well. For simplicity, our primary analysis examines workday lunch choices. We report analogous results for dinner and non-workdays in the Online Appendix.

Four sets of results emerge. First, we estimate a price elasticity of dining choice of about -1.6, which aligns well with existing estimates in the food/restaurant sector that range between -3.5 and -0.8 (e.g., Nevo, 2001; Andreyeva, Long, and Brownell, 2010; Backus, Conlon, and Sinkinson, 2021). Second, conditional on dining out, higher micro temperatures at a restaurant are associated with a reduced likelihood of being chosen. Specifically, we estimate a consumer willingness to pay (WTP) of 0.76 yuan (or about 4.2% of the price of the average meal) for a 1°C reduction in micro temperature while dining. Third, ecological features, such as urban green spaces and waterways, are positively valued in dining choices. Fourth, though not the main focus of this paper, we find robust evidence that air pollution—another environmental hazard that exhibits substantial fine-scale variability—also influences dining choices, while precipitation does not appear to have a significant effect—likely because precipitation vary less across cities, and primarily affects the extensive margin of whether to dine out at all, rather than the choice of dining location.

Our counterfactual simulations leverage the structural demand model to evaluate the consequences of uneven urban warming and the economic value of adaptation infrastructure. When we simulate a localized 1°C increase in temperature at each restaurant, holding conditions elsewhere constant, we find that average daily lunch revenue declines by ¥122 per restaurant, with larger losses concentrated among higher-priced and more competitive establishments. These effects explain 60% of the micro temperature-revenue effects that we estimate in our reduced-form analysis. In a separate counterfactual, we estimate the value of urban green space: eliminating surrounding greenery reduces daily lunch revenue by an average of ¥165 per restaurant. Aggregating across the city, the revenue generated by existing green space is several times larger than the cost of its provision, yielding a benefit–cost ratio of approximately 3. These findings quantify both the risks of localized heat and the returns to natural capital in urban adaptation policy.

Climate change is among the most urgent global crises, and its impacts are increasingly understood to be nuanced and geographically differentiated (Dell, Jones, and Olken 2014; Desme and Rossi-Hansberg, 2024). In particular, urban heat islands—where built-up areas are significantly hotter than their surroundings—now pose a major public health risk, causing more annual deaths than any other weather-related hazard (Hsu et al., 2021). Climate change is compounding these risks: global urban exposure to dangerous heat has nearly tripled since the 1980s, with city warming from urban heat islands accounting for over half of that increase (Tuholske et al., 2021). The economic relevance, however, remains poorly understood. To the best of our knowledge, our paper is among the first to quantify urban microclimate as a distinct source of economic risk. The closest related work is Colmer et al. (2023), who examine health impacts of urban heat and find that a hot day leads to significantly higher mortality in heavily paved city neighborhoods. Our contribution complements theirs by demonstrating the sizeable economic losses attributable to urban microclimate variation.

A second contribution of our paper is a practical framework for empirically quantifying consumer adaptation to microclimate risks. Adaptation is widely regarded as a crucial part of climate change strategy (Barreca et al., 2016; Carleton et al., 2022). However, measuring behavioral adaptation in real time has been challenging. We leverage detailed consumer transaction data to observe how individuals adjust their activity in response to local heat, and we estimate these responses through a canonical discrete choice modeling approach (e.g., Berry, Levinsohn, and Pakes, 1995). This approach allows us to capture substitution patterns and willingness-to-pay for microclimate resilience in a manner analogous to studies of energy and vehicle choices (e.g., Jacobsen, 2013; Ito, 2014), and enables us to recover to our knowledge the first revealed preference estimates of willingness-to-pay for microclimate comfort. This approach also yields a monetary valuation of urban climate amenities and gauges the effectiveness of ecological infrastructure in mitigating heat exposure (e.g., the cooling benefits of parks and waterways).

Finally, our study speaks to the emerging literature on firm strategy under environmental and climate-related risks. A growing body of finance and management research shows that exposure to climate risk can materially affect firm performance and behavior (Krueger, Sautner, and Starks, 2020). We find novel evidence of a substitution effect in consumer activity: on hot days, people reallocate their restaurant trips toward locations offering more favorable

microclimates (e.g. cooler temperatures, greenery or water amenities). In effect, businesses situated in more heat-resilient locales gain a competitive advantage in extreme weather, whereas those in "hot spots" experience losses. This represents an overlooked dimension of urban business strategy. Location decisions traditionally hinge on factors like market access and cost efficiency; our findings suggest that microclimate resilience is also a key determinant of sustainable performance.

Before proceeding, we highlight several important questions emerging from our analysis. First, while our study focuses on short-term, daily variability in microclimate, it raises the question of whether permanent differences in microclimate play a significant role in shaping long-term health and economic outcomes. Second, new technologies may offer innovative ways of microclimate risk adaptation. For instance, door-to-door delivery services are becoming increasingly prevalent in cities worldwide. While our adaptation analysis focuses exclusively on choices conditional on dining out, it remains an open and important question how the availability of delivery services alters the impact of microclimate risks and how the associated burdens are distributed across stakeholders.

Section 2 continues with institutional background and data description. Section 3 describes the reduced form analysis of micro temperature responses. Section 4 analyzes consumer adaptation. Section 5 conducts counterfactual analyses. Section 6 concludes.

2. Background and Data

2.1 Study Context

Guangzhou—the setting of our study—exhibits several features that inform our research design. First, it is a large subtropical metropolis in southern China with climatic and demographic characteristics well-suited to examining heat exposure. The city is a major economic center of China with a population of approximately 19 million and an annual per capita GDP around US$22,900. Summers are hot and humid, with average daily temperatures about 28.5°C, which makes the city prone to heatwaves. Rapid urbanization and dense economic activity have amplified the urban heat island effect, leading to pronounced intra-city temperature variations.

Second, Guangzhou's urban landscape is distinguished by abundant greenery and water features as a result of long-term ecological investments. The city lies along the Pearl River Delta and has, over decades, developed extensive urban forests and preserved wetlands through proactive ecological management. The municipal government has actively expanded parks and green spaces (notably under the Guangzhou Urban Green Space System Planning, 2010–2020) and created artificial lakes and waterways to enhance the urban environment. This unique combination of dense development with significant green and blue infrastructure provides a natural setting to evaluate the benefits of such adaptation measures. In our analysis, we pay particular attention to these two major "green and blue" initiatives—the city's green space expansion plan and the construction of artificial water bodies—as they offer policy-driven variation to assess how ecological investments can mitigate local climate stress.

Third, the service sector in Guangzhou accounts for over 70% of the city's GDP—significantly higher than the national average. Service-based economies are typically more urbanized and reliant on infrastructure, making them more immediately vulnerable to climate events compared to heavier industries, which can absorb shocks over longer timeframes. In particular, Guangzhou's restaurant sector is exceptionally vibrant. The city hosts over 100 restaurants per 10,000 residents—the highest density of food establishments in China. By 2019, Guangzhou's restaurant industry generated roughly 127 billion yuan in revenue. Furthermore, according to the *Guangzhou Blue Book: International Trade Center Development Report (2019)*, average annual per capita restaurant expenditure in Guangzhou exceeded US$1,000 in 2018, ranking first among Chinese cities. This vibrant dining market offers a rich setting to observe how consumers and businesses adapt to localized environmental conditions, as restaurant activity is inherently sensitive to weather and amenity variations.

2.2 Data

Restaurant transactions. We use a high-frequency dataset of restaurant transactions sourced from a leading digital payment platform in China. The data cover the period 2018–2019 and include detailed transaction records from approximately 150,000 small- and medium-sized dining establishments in Guangzhou. Over the two-year sample, the platform processed more than 1.4 billion restaurant transactions, with restaurant-related sales exceeding 45 billion RMB.

Based on official statistics for Guangzhou—reporting per capita food and restaurant spending of around 7,100 RMB for the period—our dataset captures roughly 40% of total transaction value in the city's restaurant sector. Each transaction includes information on a unique merchant identifier, a consumer-level identifier, the transaction amount, precise geolocation, and a timestamp. These granular features enable us to track restaurant-level business performance over time and to analyze individual consumer dining patterns across space. Figure 1A maps the spatial distribution of restaurants captured in our dataset, illustrating the platform's comprehensive geographic coverage.

Temperature. We measure local temperature using the ISU Global Seamless 1 km Resolution Daily Land Surface Temperature dataset (Zhang et al., 2021). This remote-sensing dataset (henceforth the ISU temperature data) is based on MODIS Land Surface Temperature product and provides daily land surface temperatures at a 1×1 km resolution and includes two observations per day (mid-day and mid-night). We average the mid-day and midnight readings to produce a daily mean temperature for each location in the city. In Appendix Figure 1, we compare the ISU data with records from fourteen *in-situ* weather monitoring stations located within or up to 30 km from the Guangzhou city boundary, and find these two data provide highly consistent measurements.

Pollution. We use $PM_{2.5}$ concentration data from the ChinaHighAirPollutants (CHAP) dataset (Wei et al., 2020; 2021). This dataset is constructed by combining multiple information sources—ground monitoring stations, satellite remote sensing, atmospheric reanalysis outputs, and chemical transport models—using machine learning to generate modeled pollution estimates at a 1×1 km resolution across China. We include $PM_{2.5}$ as a control variable in our reduced form analysis to isolate the impact of temperature from the influence of air pollution, since poor air quality could independently affect restaurant attendance and consumer well-being. In our structural estimation, we examine the separate effect of pollution as it also exhibits substantial within-city variability as temperatures do.

Precipitation. We collect daily precipitation data as a measurement for rainfall, which is another weather factor that can influence economic activity. Our source is the HRLT high-resolution precipitation dataset (Qin et al., 2022), which provides gridded daily rainfall across

China. This dataset was created by interpolating observations from national weather stations down to a spatial scale of 0.5° resolution.

Green space. To capture spatial variation in urban greenery, we digitized and georeferenced the official Guangzhou Urban Green Space System Planning (2010–2020) map. This provides a detailed delineation of areas designated for green space expansion under the city's policy plan. From this, we calculate the share of land area in each location that was planned to be green space. Among grid cells containing any planned green space, the average intended green coverage is about 15.8%. Appendix Figure 2 illustrates the original planning map.

Surface water bodies. To measure surface water bodies in the city, we use the JRC Monthly Water History dataset (version 1.4), which records surface water presence at a 30 m × 30 m resolution. We obtain monthly water classification maps for our study period (January 2018 through December 2019) and identify all grid cells that are ever classified as water during this interval. The resulting variable measures the presence of lakes, rivers, or other significant water bodies near each restaurant location. Similar to green space, this "blue infrastructure" is a key adaptation feature: it can moderate local temperatures through evaporative cooling and may attract consumers seeking comfort, so we will analyze how proximity to water mitigates microclimate risks.

Geography. Because our data come from diverse sources, we harmonize them on a common spatial framework for analysis. We divide the entire city into uniform hexagonal grid cells with 1 km sides (roughly 0.86 km² area each) and aggregate or assign all variables to this grid. Each restaurant in the transaction data is mapped to its containing hexagon, and we compute daily values of temperature, pollution, and precipitation for each hexagon using the 1 km environmental data described above. For the policy variables, we calculate the share of each hexagon's area that falls under planned green space and surface water body. Appendix Figure 3 presents summaries of key environmental variables across these grid cells (temperature, $PM_{2.5}$, precipitation, planned green space share, and water body share).

3. Microclimate Impact

3.1 Microclimate Measurement

Macro temperature (citywide average). We define macro temperature as daily citywide average temperature – a measure of the overall climate on each day. Figure 2A documents the macro-level temperature patterns using both historical records and our study-period data. The left plot of Figure 2A shows the city's annual average daily temperature from 1970 through 2024, based on NOAA National Centers for Environmental Information data. A clear trend of warming is evident: the fitted median spline shows a steady increase in Guangzhou's mean temperature over the past half-century. The right plot of Figure 2A shows the distribution of daily citywide average temperatures during our 2018–2019 study period. Guangzhou's daily mean temperatures range from roughly 4°C (39.2°F) on the coolest days to about 32°C (89.6°F) on the hottest days. This broad range indicates substantial day-to-day and seasonal variability in macro temperatures, providing the backdrop for our microclimate analysis.

Micro temperature shock (localized deviations). We capture microclimate shocks as localized temperature differences across the city. Using the 1 km-resolution ISU gridded temperature data, we compute each 1 km hexagonal cell's daily temperature and subtract the citywide mean (i.e., the macro temperature) for that day; this difference is what we call the micro temperature shock for that location. Figure 2B illustrates the extent of these micro-level temperature variations. The left map in Figure 2B plots each 1 km hexagonal grid's average temperature deviation from the daily city mean (for 2018–2019), with some areas of the city are consistently warmer than the citywide average (positive deviations), while others are consistently cooler (negative deviations). These persistent microclimate differences span on the order of a few degrees Celsius.

The right panel of Figure 2B further quantifies microclimate variability conditional on the macro temperature. Here, we group days by the citywide average temperature (in 5°C bins) and plot the distribution of grid-level, micro temperatures within each bin. The resulting curves show that even after accounting for the day's general weather (the macro temperature), considerable microclimate heterogeneity remains across the city. Figure 2 highlights the distinction between

macro and micro temperatures: the city experiences both broad shifts in overall climate and fine-grained local deviations on any given day, which we will focus on in our subsequent analysis.

3.2 Estimation Framework

We begin with a flexible reduced-form empirical strategy to quantify how micro temperature variation affects weekly restaurant performance. We estimate a regression of weekly store-level outcomes on the distribution of daily temperature realizations across 1°C temperature bins, controlling for time-invariant store characteristics and common time shocks. Our regression specification is:

$$Y_{jw} = \sum_b \beta^b \cdot \#\text{Days}(\text{TempBin} = b)_{g_j w} + \mathbf{X}_{g_j w} \cdot \gamma + \eta_j + \eta_w + \epsilon_{jw}$$

where Y_{jw} denotes the outcome variable for store j in week w, and $\#\text{Days}(\text{TempBin} = b)_{g_j w}$ is the number of days in week w that the local temperature (in the 1 km grid g containing store j) falls into 1°C temperature bin b. The two primary outcomes we analyze are weekly transaction volume (number of customer transactions, in log) and weekly revenue (total sales, in log). The term $\mathbf{X}_{g_j w}$ includes analogous counts of days with specific pollution levels and precipitation levels, which serve as control variables for other environmental conditions. We also include store fixed effects (η_j) to absorb all time-invariant differences across stores (e.g. location, average customer flow, or baseline climate) and week fixed effects (η_w) to control for any citywide temporal shocks – including macro temperature – or seasonal patterns affecting all stores in a given week. ϵ_{jw} is the error term and we cluster standard errors at the store and week level.

We omit the 19-20°C bin (around 66.2°F) from the regression, treating it as the baseline category against which all other temperature effects are measured. This moderate temperature range is thus normalized to zero effect. So, each coefficient β^b is interpreted as the incremental effect of having one additional day in temperature bin b instead of a day in the reference bin, holding the distribution of other bins constant. In other words, β^b captures the change in weekly transactions or revenue when a single day at around 19–20°C is hypothetically replaced by a day in bin b, controlling for all other factors, including the remaining days' temperatures, pollution and rain controls, and fixed effects. Because the outcomes are in log form, these coefficients can

be read as approximate percentage changes in the weekly outcome relative to the baseline temperature conditions.

Our identification of the temperature impact leverages two sources of variation in the data. First, by using store (location) fixed effects, we isolate within-store temporal variation: comparisons of the same store's performance in hotter versus cooler weeks. Second, by including week fixed effects, we exploit cross-store spatial variation within each week: in a given week, some neighborhoods are hotter than others, and those differences can be linked to differences in outcomes across stores. By differencing out each store's average performance and each week's overall shocks, the coefficients β^b are identified from deviations in local temperature beyond a store's usual climate and beyond the citywide weekly average. This design ensures that microclimate shocks (local temperature fluctuations) are driving the estimated effects. As a result, our estimates reflect the impact of granular temperature differences on restaurant metrics, net of any broader time trends or unobserved store traits.

3.3 Main Results

Figure 3 plots the estimated β^b coefficients for each micro temperature bin, with the [19°C, 20°C) range serving as the reference point. The results reveal a pronounced nonlinear relationship between local temperature and restaurant performance. In both the transaction volume and revenue specifications, coefficients near the comfortable reference temperature are close to zero, whereas the losses to business outcomes accelerate as heat intensifies. Moderate heat (just above 20°C) induces only modest declines, but the negative impact grows substantially larger for extreme heat levels.

The magnitude of the effect is economically significant, especially at the upper end of the temperature range. For example, replacing one temperate day in the 19–20°C range with an extremely hot day (≥30°C, or 86°F) leads to approximately a 7.3% decrease in weekly transaction volume for that store. In absolute terms, an average restaurant in our data would experience on the order of 47 fewer transactions over the week due to that single day of extreme heat. Similarly, weekly revenue drops by about 6.4% under the same temperature shift, which corresponds to roughly ¥1,400 (or $192) less in sales for the week. These findings thus suggest that high micro

temperatures can substantially depress both the number of customer visits and the total sales at the store-week level. Notably, the estimates for revenue closely mirror those for transaction counts, implying that the reduction in sales is primarily driven by fewer transactions, rather than a large drop in spending per transaction.

We reiterate that these results underscore that it is the neighborhood-level temperature anomaly – over and above the citywide average heat – that drives the adverse business outcomes. In other words, even after accounting for a day's overall temperature in the city, localized microclimate shocks exert a substantial independent influence on restaurant sales. Appendix Figure 4 presents robust results from the daily-level analysis, while Appendix Figure 5 illustrates heterogeneity in responses to microclimate temperature.

3.4 Mechanisms

One potential channel for the observed revenue decline is a supply-side adjustment: restaurants may choose to close operations on exceptionally hot days, directly reducing the capacity to transact. To investigate this mechanism, we analyze whether restaurants are more likely to be closed for business on hotter days, using the same microclimate variation framework as in our main analysis. The empirical strategy leverages week-by-week fluctuations in local temperature: we estimate how substituting a mild day with an extremely hot day (holding other factors constant with store and week fixed effects) affects the number of days the restaurant remains closed that week.

Figure 4 presents the estimated change in weekly closure days as a function of daily microclimate temperature bins. The pattern provides clear evidence of a modest supply-side response to heat. The black line in the figure indicates how the probability of a restaurant closing rises with extreme temperature: as temperatures approach the highest bins, the number of closed days per week ticks upward slightly above the baseline. In particular, relative to a temperate day in the 19–20°C range (the reference bin), an extremely hot day of ≥30°C leads to an increase of about 0.053 closure days per week – that is, 5.3% of one business day. This estimate implies that restaurants do shut down slightly more often during heatwaves. The effect is relatively modest: an extra hot day would cause the average restaurant – which handles roughly 92 transactions per

day and about ¥3,107 in daily revenue – to forgo on the order of 5 transactions and ¥165 in sales that week due to the added closure time.

We can compare this supply-side impact to the overall business losses from heat in order to gauge its importance. From our damage function estimates in Figure 3, replacing a mild day with a ≥30°C day reduces weekly customer traffic by about 7.3% (roughly 47 fewer transactions) and weekly revenue by 6.4% (approximately ¥1,400). The closure effect quantified above – about 5 fewer transactions and ¥165 down – explains on the order of 11% of the total drop in transactions and 12% of the revenue decline attributable to that hot day. In other words, the bulk of the revenue shortfall on extremely hot days must come from within-day reductions in activity while restaurants are open. Appendix Figure 6 shows no significant response in price or discount per revenue.

Another potential channel is a demand-side response: consumers may choose not to dine out (extensive margin) or may reduce their expenditure when they do (intensive margin), particularly on exceptionally hot days. To conduct a consumer-level analysis, we randomly sample 10,000 consumers and successfully identify each individual's dining hub to measure their experienced microclimate temperature. Details of the sample construction are provided in Section 4.2. To ensure estimation precision, we group temperatures into 2-degree bins.

Figures 5A and 5B display the changes in the weekly probability of dining out and the log of consumer expenditure, respectively, as functions of microclimate temperature bins (measured as the average temperature in lunch and dinner hub centers). Compared to a temperate day in the 18–20°C range (used as the reference category), an extremely hot day (⩾30°C) leads to a 1.4% decrease in the likelihood of dining out and a 1.9% reduction in weekly out-of-pocket expenditure per consumer.

On average, each restaurant attracts about 450 consumers per week, and each consumer generates approximately ¥80 in weekly expenditure. Thus, the decrease on the extensive margin translates to a weekly revenue loss of around ¥504, while the intensive margin results in a loss of about ¥684. Combined, these effects account for roughly 85% of the observed revenue decline—a pattern that holds similarly for weekly transaction volumes.

This evidence suggests that while supply-side adjustments may exist, the majority of the drop in transactions and revenue during hot weather stems from changes in consumer behavior. In the next section, we examine these demand-side adaptation mechanisms in greater detail, exploring how consumers adjust their dining patterns in response to microclimate extremes and whether such adaptations help mitigate the impacts on restaurant business outcomes.

4. Consumer Adaptation

4.1 Microclimate and the Urban Environment

In dense urban areas like Guangzhou, pockets of greenery and surface water tend to remain cooler than surrounding built-up neighborhoods due to shade, evapotranspiration, and evaporative cooling. These green and blue urban spaces effectively act as natural air conditioners, mitigating extreme local heat (e.g., Gunawardena, Wells, and Kershaw, 2017). We empirically document how such ecological features measurably moderate the local microclimate by combining temperature observations with spatial data on the city's green spaces and waterways.

Figure 6 illustrates the distribution of urban ecological features in Guangzhou and their cooling influence on local temperatures. Panel A maps the city's green and blue infrastructure, including designated green spaces (left map, in green) and surface water bodies (right map, in blue). Panel B of Figure 6 quantifies how these features moderate neighborhood thermal conditions. The left graph plots each grid's average daily microclimate temperature shock – defined as the grid's average deviation from the citywide macro temperature – against its distance to the nearest green space. The right graph shows an analogous plot for distance to the nearest waterway. In both cases, a clear positive relationship emerges: proximity to vegetation and waterways significantly reduces a location's temperature extremes, providing a tangible cooling benefit at the micro scale.

Figure 7 demonstrates how the presence of greenery and water correspond to business performance on hot days. Panel A compares the micro temperature-revenue response function in areas with abundant vegetation versus those with sparse vegetation. We split the sample by local greenness: restaurants in the greenest one-third of locations (high tree/park cover) vs. those in the bottom third. Each series in the figure shows how log weekly revenue changes as local microclimate temperature rises. Consistent with the cooling effect of vegetation, the revenue of

businesses surrounded by ample greenery remains relatively stable across moderate temperature increases and only modestly declines at the highest temperatures. By contrast, restaurants in areas with little nearby green cover suffer sharp drops in revenue as micro-level temperature climbs. Panel B presents an analogous comparison for water bodies: establishments near rivers or lakes (top tercile in water proximity) experience much smaller heat-related revenue losses than those far from any water (bottom tercile). These patterns suggest that the presence of urban green or blue infrastructure buffers businesses against heat stress, attenuating the economic damage of extreme hot days. We next formally model and estimate the role of these adaptive features on consumer choice.

4.2 Consumer Choice Model and Estimation

In this section, we present our empirical model for consumer restaurant choice on a single meal trip and outline the estimation strategy. We estimate consumer preferences for restaurant characteristics using a discrete choice model incorporating consumer heterogeneity, following the framework of Berry et al. (1995, 2004), Petrin (2002), Goolsbee and Petrin (2004), and Train and Winston (2007).

4.2.1 Consumer Sampling

Consumers. To credibly estimate our consumer restaurant choice model, we construct a trip-level dataset focused on consumers with frequent and consistent dining patterns. We begin by identifying consumers who restrict their dining to one restaurant per meal period – that is, at most one establishment during weekday lunch hours (11:00–14:00) and at most one during dinner hours (17:00–22:00) on any given day.[1] This filters out individuals with irregular schedules or multiple same-meal visits, so that each lunch or dinner corresponds to a single discrete choice event.

From this group of consistent diners, we further select those with the longest active spans of dining activities in our data (i.e. the greatest number of days with observed lunch or dinner visits).. Focusing on these high-frequency consumers yields a sample of intensive restaurant users

[1] The lunch and dinner hours are determined based on the distribution of business hours observed in the data as shown in Appendix Figure 7.

whose behavior can be tracked repeatedly over time. Finally, we randomly draw 10,000 consumers from this pool for our analysis to maintain a manageable sample size for our structural estimation.

A natural concern is whether our sample—restricted to high-frequency, consistent diners—is representative of the broader consumer population. To assess this, we later compare the predicted effects from our structural counterfactuals to those from reduced-form estimates. The similarity in magnitude between the two provides reassurance that, while selective, our sample captures the key behavioral patterns driving the observed aggregate effects.

Dining Hubs. We next identify each consumer's primary "dining hubs" – the focal locations from which they typically depart for lunch or dinner trips. Since variation in temperature and other environmental amenities is critical for identifying consumers' willingness to pay for these microclimate characteristics surrounding restaurants, defining these hubs allow us to specify a plausible trip origin for each meal occasion in the choice model.

To determine these hubs, we implement a data-driven clustering approach for each individual. Specifically, for each sampled consumer, we first collect all the geolocated restaurants they visited, separately for weekday lunches and for dinners, and apply the Hierarchical Density-Based Spatial Clustering of Applications with Noise (HDBSCAN) algorithm to group these locations into clusters. HDBSCAN automatically detects spatial clusters of visits without requiring a pre-specified the number of clusters. By identifying clusters of varying shapes and densities while treating infrequent, scattered visits as noise, the algorithm helps identify major clusters that likely reflect the consumer's habitual dining areas, rather than random outlier trips.

We designate the cluster with the highest number of visits as the consumer's primary dining hub for each meal period. The centroid of this primary cluster as is then defined as the consumer's trip origin for modeling purposes. In practice, this origin represents a stable anchor in the consumer's daily routine (for example, a primary lunch hub likely corresponds to a workplace vicinity, while a dinner hub corresponds to a home neighborhood). All subsequent trip-level analyses use these origin points as the starting location of the consumer's restaurant choice.

Figure 8A illustrates the result of this procedure for a sample consumer's weekday lunch trips. The figure shows distinct clusters of visited restaurants, with the centroid of the largest cluster (marked by a red star) identified as the primary lunch hub. Across our sample, most restaurant activity is concentrated in one or two such hubs per consumer. Figure 8B highlights this pattern by plotting the cumulative share of each consumer's total dining spending accounted for by their top-N hubs. We see that the top one hub alone typically captures a large majority of dining activity, and the addition of a second hub accounts for nearly all regular transactions. This strong concentration supports the validity of using each consumer's primary hub as the trip origin– it reflects the stable center of their dining behavior that our structural model exploits.

4.2.2 Restaurant Choice Model

Utility. Suppose individual i cares about the expected temperature difference between their dining hub (e.g., workplace or home) when dining at restaurant j on date t, as well as the associated cost (including travel distance and dining expenses). We assume consumers make independent choices for their dining locations. The utility function of this meal trip can be expressed as:

$$u_{ijt} = \alpha - \beta \cdot p_{jt} + \gamma \cdot \Delta\text{temp}_{ijt} + \rho \cdot \mathbf{X_{ijt}} + \lambda \cdot \text{logdist}_{ij} + \eta_j + \eta_t + \epsilon_{ijt}$$

where p_{jt} is the price (i.e., expected dining expenses) at restaurant j on date t, and $\Delta\text{temp}_{ijt} \equiv \text{temp}_{jt} - \text{temp}_{it}$ represents the expected temperature difference between store j and individual i's default dining hub location on date t (i.e., how the restaurant's local temperature deviates from that at the individual's workplace or home), $\mathbf{X_{ijt}}$ represents the difference in other environmental characteristics, such as greenery and water coverage, pollution and precipitation, between the restaurant and the dining hub on date t. logdist_{ij} is the logged travel distance between individual i and restaurant j. η_j is the mean utility of dining at restaurant j, and η_t represents fixed effects for day$t$. Lastly, ϵ_{ijt} is an i.i.d. idiosyncratic preference shock, as assumed to follow type 1 extreme value distribution. The utility of the outside option (i.e., not eating out) is given by $u_{ijt} = \epsilon_{i0t}$.

Given the utility specification above, the marginal willingness to pay (MWTP) for a unit increase in temperature difference can be derived , which is given by the ratio of the marginal utility of the temperature difference to marginal utility of income (the disutility of price):

$$\text{MWTP} = \frac{\gamma}{\beta}$$

This ratio, $\frac{\gamma}{\beta}$, represents how much the consumer is willing to pay for a one-unit increase in the temperature difference between their default location and the restaurant, such as for cooler temperatures. Essentially, it translates the utility gained from temperature difference into monetary terms, capturing the trade-off the consumer is willing to make between monetary cost and temperature difference.

Individual Choice Probability. We assume that consumer i observes all open restaurants on day t and chooses the one that maximizes her utility for a given meal. Let J_t represent the choice set, and Y_{ijt} is a dummy variable equal to 1 if consumer i choose restaurant j on date t. For simplicity, we define $\boldsymbol{\theta_1} = \{\alpha, \beta, \boldsymbol{\eta}\}$ as the set of parameters associated with individual-invariant variables, and $\boldsymbol{\theta_2} = \{\gamma, \rho, \lambda\}$ as the set of consumer-specific preference parameters. The utility components are defined as follows: $\delta_{jt}(\boldsymbol{\theta_1})$ captures the mean utility of restaurant j on date t, and $\mu_{ijt}(\boldsymbol{\theta_2})$ captures the individual-specific deviation from the mean utility. More specifically,

$$\delta_{jt}(\boldsymbol{\theta_1}) = \alpha - \beta \cdot p_{jt} + \eta_j + \eta_t + \xi_{jt}$$

$$\mu_{ijt}(\boldsymbol{\theta_2}) = \gamma \cdot \Delta\text{temp}_{ijt} + \rho \cdot \mathbf{X_{ijt}} + \lambda \cdot \text{logdist}_{ij}$$

Given the type 1 extreme value distribution of ϵ_{ijt}, the probability that the consumer chooses restaurant $j \in J_t$ on date t is

$$s_{ijt} \equiv \text{Prob}\left(Y_{ijt} = 1 \middle| \boldsymbol{\theta_1}, \boldsymbol{\theta_2}, \mathbf{p}, \mathbf{X}, \boldsymbol{\Delta}, \mathbf{logdist}\right)$$

$$= \frac{\exp\left(\delta_{jt}(\boldsymbol{\theta_1}) + \mu_{ijt}(\boldsymbol{\theta_2})\right)}{\sum_{j' \in J_t \cup \{0\}} \exp\left(\delta_{j't}(\boldsymbol{\theta_1}) + \mu_{ij't}(\boldsymbol{\theta_2})\right)}$$

Market Share. Aggregating individual choice probabilities yields the predicted market share of restaurant j on date t:

$$\hat{S}_{jt} = \int s_{ijt}(\boldsymbol{\theta_1}, \boldsymbol{\theta_2}; \mathbf{p}, \mathbf{X}, \boldsymbol{\Delta}, \mathbf{logdist}) dF(\mu_i)$$

4.2.3 Estimation

Following Goolsbee and Petrin (2004) and Train and Winston (2007), the estimation proceeds in two stages. In the first stage, we estimate the nonlinear parameters $\boldsymbol{\theta_2}$ by maximizing the likelihood function below, subject to the constraint that predicted market shares of the restaurants match the observed shares in the data. The log-likelihood function for the full sample across all time periods is given by:

$$\max_{\boldsymbol{\theta_2}} \log L(\boldsymbol{\delta}, \boldsymbol{\theta_2}; \mathbf{X}, \boldsymbol{\Delta}, \mathbf{logdist}) \equiv \sum_i \sum_j \sum_t Y_{ijt} \log s_{ijt}(\boldsymbol{\delta}, \boldsymbol{\theta_2}; \mathbf{X}, \boldsymbol{\Delta}, \mathbf{logdist})$$

$$s.t.\ \hat{S}_{jt}(\boldsymbol{\delta}, \boldsymbol{\theta_2}; \mathbf{X}, \boldsymbol{\Delta}, \mathbf{logdist}) = S_{jt}$$

Given the larger number of mean utilities $\boldsymbol{\delta}$, we follow the two-step procedure outlined in Berry et al. (1995), which shows that under certain regularity conditions, for each $\boldsymbol{\theta_2}$, there exists a unique $\boldsymbol{\delta}$ that matches the predicted market shares $\hat{S}_{jt}$ with observed ones S_{jt}.[2] We back out the mean utility vector $\boldsymbol{\delta}$ for any given $\boldsymbol{\theta_2}$ using a contraction mapping technique:

$$\delta_{jt}^{h+1}(\boldsymbol{\theta_2}) = \delta_{jt}^{h}(\boldsymbol{\theta_2}) + \ln S_{jt} - \ln \hat{S}_{jt}(\delta_{jt}^{h}, \boldsymbol{\theta_2})$$

We iterate this equation until the difference between δ_{jt}^{h+1} and δ_{jt}^{h} falls below a pre-specified inner loop tolerance. We use a strict convergence criterion of 10^{-5} to minimize the risk of convergence to a local optimum.

In the second stage, once $\boldsymbol{\theta_2}$ and $\boldsymbol{\delta}$ are estimated using maximum likelihood, we recover the linear parameters $\boldsymbol{\theta_1}$ by regressing the estimated mean utilities on the observed covariates. To address the potential endogeneity of prices, we use the share of active rival restaurants in the same food category (e.g., Chinese fast food, western food, etc.) within a 3-kilometer radius of store j on date t as an instrumental variable. This variable captures the intensity of local competition faced by store j on date t, and is assumed to be exogenous, since the opening and location decisions of restaurants occur over longer horizons. This approach is consistent with BLP-style instruments that exploit variation in the number of competing products in practice.

[2] From the City Statistics Yearbook, there were 7.54 million employed persons in private enterprises, and self-employed individuals in Guangzhou in 2018, and 77.26 million in 2019. We treat these figures as the market size for 2018 and 2019, respectively. To calculate the restaurant-daily market share S_{jt}, we divide the daily total number of distinct consumers during weekday-lunch (dinner) hours at each restaurant by these market size numbers.

$$\delta_{jt} = \alpha - \beta \cdot p_{jt} + \eta_j + \eta_t + \xi_{jt}$$

4.2.4. Identification

Consumer utility consists of a mean utility component and individual heterogeneity. The linear parameters in δ_{jt} are identified through the variation in market shares of restaurants on date t corresponding to daily variation in price and other observed restaurant characteristics. Due to the potential endogeneity between price and the unobserved restaurant quality ξ_{jt}, we use the number of closely competing restaurants in the nearby neighborhood as instruments to capture exogenous variation in prices. These instruments reflect the intensity of competition and help address the endogeneity concern.

The price coefficient enables us to infer the consumer's marginal utility of income, which in turn allows us to recover their willingness to pay for cooler temperatures and improved environmental amenities. The nonlinear parameters $\boldsymbol{\theta_2} = \{\gamma, \rho, \lambda\}$ in the individual heterogeneity component are identified through the interaction between temperature and other environmental conditions in the consumer's dining hub and those at the chosen restaurant. For example, if consumers located in hotter areas disproportionately choose restaurants situated in cooler environments, we would expect a significant coefficient on the temperature deviation variable. Additionally, when the temperature surrounding a restaurant increases, consumers may substitute toward restaurants in relatively cooler areas—this substitution behavior helps identify the temperature deviation parameter and consumer's micro-scale adaptation. Similarly, if consumers whose workplaces lack greenery are more likely to dine at restaurants surrounded by urban greens, we would expect a positive and significant coefficient on the greenery deviation variable. Finally, regardless of where they live, consumers tend to favor nearby restaurants; thus, we would expect λ, which captures the disutility of travel distance, to be negative and significant.

4.3 Consumer Choice Results

Table 1 presents the structural estimates of the discrete choice model. As expected, conventional cost factors strongly influence dining decisions: consumers are less likely to spend in restaurants that are farther from their usual dining hub or that charge higher prices. The implied own-price elasticity of restaurant choice is close to -1.6, which generally align with prior estimates for the restaurant industry (e.g., Nevo, 2001; Andreyeva, Long, and Brownell, 2010;

Backus, Conlon, and Sinkinson, 2021). These cost sensitivities confirm that the model captures economically meaningful behavior and set the stage for evaluating trade-offs with environmental amenities.

We find that a higher local temperature at a restaurant significantly deters consumer choice. The coefficient on the micro temperature difference (between the restaurant and the consumer's default, primary dining hub location) is negative and significant, indicating that when a restaurant's surrounding temperature is higher, consumers are less likely to choose it and instead substitute toward cooler alternatives. Combining this effect with the estimated marginal utility of income (price coefficient), we estimate that consumers are willing to pay approximately 0.7–0.9 yuan for a 1°C reduction in dining temperature. This microclimate sensitivities substantial—it explains roughly 60% of the decline in restaurant visits on the extremely hot days (≥30°C) observed in our reduced-form analysis. Thus, a significant share of the microclimate burden is mitigated through adaptive behavior: when temperatures rise, consumers partially offset the comfort loss by shifting toward cooler restaurants.

Urban green and blue infrastructure further shape consumer preferences. Table 1 shows that restaurants located in areas with more green space or near bodies of water tend to attract more customers. Our estimates imply that an additional square kilometer of urban green space in the vicinity of a restaurant increases a representative consumer's utility by an amount equivalent to roughly ¥3.7 per lunch trip. This result highlights the significant direct amenity value of urban greening—likely due to aesthetic or recreational appeal. The effect of nearby water bodies (lakes, rivers, or ponds) is also positive in simpler models, but is less stable than the greenery effect. In our richest specification (e.g. when we include micro temperature, green space, and water measures simultaneously), the estimated effect of waterways becomes imprecise. This could stem from collinearity or measurement issues: green spaces and waterways often coincide spatially, making it difficult to disentangle their individual contributions. It may also reflect temporal variation in the appeal of water features (e.g. seasonal differences in the use of waterfront areas). The upshot is that while there is suggestive evidence consumers value proximity to water, the magnitude of the water amenity effect should be interpreted with caution. In contrast, the estimates on green infrastructure is consistently positive and robust.

Our model also allows for other environmental factors. Local air quality significantly affects restaurant choice: higher $PM_{2.5}$ pollution at a given location deters consumers, even after controlling for other attributes. On the other hand, precipitation has little to no impact on restaurant selection once the decision to dine out has been made. This is perhaps intuitive—rain is more of a city-wide event, and likely primarily impacts the extensive margin (whether to go out) rather than the intensive margin of which restaurant to visit.

One potential concern is that consumers, when making dining decisions, may consider not only the temperature difference between the hub center and the restaurant, but also the overall temperature along the travel route. To address this possibility and complement our benchmark analysis, we construct a measure of on-route temperature through the following steps: First, for each hub center–restaurant pair, we obtain the most time-efficient route using the Baidu Map platform, a leading map service provider in China. Second, we map each route onto the hexagonal temperature grid and identify all the hexagons it intersects. Finally, we calculate the average temperature across these intersected grids to define the on-route temperature. Appendix Figure 8A shows the distribution of shortest travel time routes, which align well with the road network data. Appendix Figure 8B provides an illustrative example of the route mapping and temperature calculation. Table 2 reports the results using the on-route temperature measure, which are consistent with our benchmark findings based on hub-to-restaurant temperature differences.

In Appendix Table 2, we report a parallel analysis of dinner choices, which reveals similar behavioral patterns to those observed at lunch. Consumers likewise tend to avoid hot, distant, and polluted locations in the evening, while preferring greener areas. The estimated coefficients are comparable in both sign and magnitude to the lunch results. Appendix Table 3 presents results from specifications that include interaction terms between temperature differences and ecological characteristics. These results suggest that urban ecological features help mitigate the disutility associated with high microclimate temperatures. We also explore consumers' flexibility in adapting to temperature variation from the perspective of transport accessibility. Appendix Table 4 shows that consumers located near bus stations exhibit greater sensitivity to temperature differences, possibly because proximity to public transport facilitates spatial reallocation and adaptive behavior.

The structural estimates align with the reduced-form evidence of microclimate adaptation discussed earlier. In our reduced-form analysis, we observed that restaurants surrounded by greenery or water experienced smaller revenue losses on hot days, relative to those in less buffered areas (see Figure 7). The discrete choice model estimation now provides the underpinning for that pattern: consumers actively shift toward the thermally comfortable (green or water-abundant) locations, as a coping strategy during periods of heat stress.

Our results demonstrate that micro-scale adaptation is already occurring through individual choices, where consumers modulate their behavior by seeking out microclimate refuges—cooler micro-environments and ecologically rich locales—even if it means incurring higher prices or longer travel. By quantifying these preferences, we not only confirm that consumers value microclimate improvements, but also provide a basis for valuing urban climate adaptation initiatives. The next section builds on these findings to evaluate the broader implications of microclimate change and the potential welfare gains from the city's urban green space construction.

5. Microclimate Change Burden and Adaptation Value

We now leverage our structural model to conduct counterfactual simulations of microclimate changes. This approach moves beyond reduced-form correlations by explicitly modeling how consumers substitute across restaurant locations with different amenities (e.g., cooler, greener areas) when conditions change. We focus on the economic consequences of rising urban heat and the protective value of climate adaptation infrastructure. In particular, we consider two scenarios: (1) a local temperature increase to evaluate the burden of localized urban warming, and (2) the removal of urban greenery to assess the business value of cooling amenities provided by green infrastructure.

5.1 Increase in Micro Temperature

To evaluate the effect of microclimate on business outcomes, we use the estimated demand model to simulate a 1°C rise in the local temperature at each restaurant location (one at

a time), holding all other conditions fixed. This counterfactual isolates the effect of localized heat on a restaurant's own performance, allowing consumers to freely substitute to to unaffected (cooler) alternatives. Figure 9A reports the distribution of revenue losses under this 1°C microclimate warming shock. Virtually all establishments experience a downturn in sales when their immediate environment gets hotter. The average loss is about 122 yuan per day (roughly a 12% decline in lunchtime revenue). The distribution of losses is broad: while many restaurants see modest declines, a non-trivial subset experience quite severe revenue drops under a 1°C local warming, underscoring that the burden of rising heat can be substantial for certain businesses.

Figure 9B explores the heterogeneity of these losses by store and neighborhood characteristics. The revenue hit from a hotter microclimate is more pronounced for higher-revenue and higher-priced restaurants. Likewise, restaurants located in areas with denser local competition within a 3 km radius suffer larger losses. In more competitive neighborhoods, consumers can more easily substitute away to nearby rivals when a particular restaurant becomes uncomfortably hot.

This setting also provides a direct comparison between our structural predictions and the reduced-form estimates of heat's impact. The structural model implies that replacing a temperate day with an extreme hot day (≥30°C) reduces an average restaurant's weekly revenue by roughly ¥850, which is on the order of 60% of the ≈¥1,400 weekly loss estimated from the reduced-form analysis. The close alignment in magnitude suggests that the behavior of these frequent diners in our structural sample closely mirrors that of the broader customer base driving the aggregate effects. The remaining gap in magnitude likely reflects adaptation along the extensive margin – customers who choose not to dine out at all (or switch to home delivery) on very hot days – which is beyond the scope of our model that conditions on the decision to dine out.

5.2 Value of Urban Green Space

We evaluate the protective value of urban green infrastructure by simulating a counterfactual scenario with no greenery surrounds restaurants. Specifically, we set each location's surrounding green coverage to zero and use the structural model to predict business outcomes in the absence of parks or tree cover. Comparing this "no-green" scenario to the status

quo reveals the economic gains attributable to Guangzhou's urban ecological investments (Section 2.1). Figure 10A shows the distribution of revenue changes when moving from a zero-green environment to the actual greenery levels. On average, a restaurant's daily lunch-hour revenue is about 165 yuan higher with the presence of nearby green space than it would be with no green at all – roughly a 16% increase over baseline sales. This positive effect reflects both the direct amenity value of greenery (attracting customers with a more pleasant setting) and its indirect cooling effect on local microclimates. The distribution of revenue gains is again wide: while many establishments enjoy moderate boosts, those surrounded by extensive greenery enjoy particularly large increases.

Figure 10B furthers examines the heterogeneity in these greenery-derived gains across restaurant types and locations. The pattern mirrors the results from the micro-heat-shock simulation. Higher-revenue venues reap larger absolute gains from urban green space. Restaurants with higher menu prices also tend to benefit more from greenery, perhaps consistent with clientele at upscale establishments valuing a comfortable environment disproportionately more. Moreover, businesses in highly competitive areas see greater gains from nearby green amenities. In dense restaurant clusters, an attractive microclimate created by urban greenery can be a differentiating factor that draws customers, conferring a competitive edge. These heterogeneity results suggest that the same factors which exacerbate losses under heat stress — large scale of operations and abundant substitutes — also amplify the gains from adaptation features like greenery.

This counterfactual exercise provides a valuation of natural capital in the urban context. The estimated 165 yuan daily boost per restaurant translates into substantial aggregate benefits citywide. For perspective, given Guangzhou's restaurant sector annual revenue of roughly 127 billion yuan, the existing urban green infrastructure can be inferred to contribute on the order of 20 billion yuan in extra revenue per year. Comparing this benefit to the city's investment in green projects (about 6.6 billion yuan over the past decade) implies a benefit-cost ratio of around 3 for Guangzhou's urban greenery initiatives. In effect, our structural simulations monetize the value of climate-mitigating infrastructure: they demonstrate that urban parks, trees, and wetlands yield high economic returns by bolstering business activity and resilience in the face of rising heat. This provides a practical framework for natural capital valuation, linking ecological investments to measurable gains in economic performance.

6. Conclusion

Microclimate variations can have economically significant effects on urban consumer behavior and business performance. Hotter neighborhoods experience noticeable downturns in restaurant foot traffic and revenue, while cooler areas with ample green or blue infrastructure fare comparatively better. We show that consumers actively adapt to high temperatures by shifting their dining trips toward more comfortable (cooler and greener) locations, which in turn mitigates a substantial share of the potential losses from extreme heat. By incorporating this adaptive behavior into a structural model of restaurant choice, we are able to quantify the protective value of urban natural capital: features such as parks, tree canopy, and waterways serve as local climate buffers that meaningfully bolster consumer welfare and sales in hot conditions.

Our study highlights the economic returns to investments in urban climate resilience. The evidence suggests that city-led initiatives to expand green infrastructure can pay dividends by both enhancing day-to-day consumer experience and strengthening the local economy's resilience to rising heat stress. From a cost-benefit perspective, the existing green spaces in our study city generate several-fold greater economic benefits in consumer spending than the cost of their provision, underscoring a high return on investment. More broadly, by documenting sizable gains from micro-scale adaptation measures, we make the case that urban planners and businesses should treat microclimate management as an integral component of strategies to combat climate risks. These insights can inform adaptation policies in rapidly warming cities, illustrating that even relatively localized interventions – increasing tree cover, creating parks, or preserving water bodies – can have outsized effects on economic resilience in the face of global climate change.

References

Andreyeva, Tatiana, Michael W. Long, and Kelly D. Brownell. "The impact of food prices on consumption: a systematic review of research on the price elasticity of demand for food." American Journal of Public Health 100, no. 2 (2010): 216-222.

Backus, Matthew, Christopher Conlon, and Michael Sinkinson. Common ownership and competition in the ready-to-eat cereal industry. No. w28350. National Bureau of Economic Research, 2021.

Barreca, Alan, Karen Clay, Olivier Deschenes, Michael Greenstone, and Joseph S. Shapiro. "Adapting to climate change: The remarkable decline in the US temperature-mortality relationship over the twentieth century." Journal of Political Economy 124, no. 1 (2016): 105-159.

Berry, Steven, James Levinsohn, and Ariel Pakes. 1995. "Automobile Prices in Market Equilibrium." Econometrica 63 (4): 841–890.

Berry, Steven, James Levinsohn, and Ariel Pakes. 2004. "Differentiated products demand systems from a combination of micro and macro data: The new car market." Journal of Political Economy 112 (1): 68–105.

Carleton, Tamma, Amir Jina, Michael Delgado, Michael Greenstone, Trevor Houser, Solomon Hsiang, Andrew Hultgren et al. "Valuing the global mortality consequences of climate change accounting for adaptation costs and benefits." The Quarterly Journal of Economics 137, no. 4 (2022): 2037-2105.

Colmer, Jonathan, Tridevi Chakma, and John Voorheis. 2023. "The Causes and Consequences of Urban Heat Islands." Working Paper

Dell, Melissa, Benjamin F. Jones, and Benjamin A. Olken. 2014. "What Do We Learn from the Weather? The New Climate–Economy Literature." Journal of Economic Literature 52 (3): 740–798.

Desmet, Klaus, and Esteban Rossi-Hansberg. 2024. "Climate Change Economics over Time and Space." Annual Review of Economics 16 (forthcoming).

Goolsbee, Austan, and Amil Petrin. 2004. "The consumer gains from direct broadcast satellites and the competition with cable TV." Econometrica 72 (2): 351–381.

Gunawardena, Kanchane R., Martin J. Wells, and Tristan Kershaw. "Utilising green and bluespace to mitigate urban heat island intensity." Science of the Total Environment 584 (2017): 1040-1055.

Hsu, Angel, Glenn Sheriff, Tirthankar Chakraborty, and Diego Manya. "Disproportionate exposure to urban heat island intensity across major US cities." Nature Communications 12, no. 1 (2021): 2721.

Ito, Koichiro. "Do consumers respond to marginal or average price? Evidence from nonlinear electricity pricing." American Economic Review 104, no. 2 (2014): 537-563.

Jacobsen, Mark R. "Fuel economy and safety: The influences of vehicle class and driver behavior." American Economic Journal: Applied Economics 5, no. 3 (2013): 1-26.

Krueger, Philipp, Zacharias Sautner, and Laura T. Starks. "The importance of climate risks for institutional investors." The Review of Financial Studies 33, no. 3 (2020): 1067-1111.

Nevo, Aviv. "Measuring market power in the ready-to-eat cereal industry." Econometrica 69, no. 2 (2001): 307-342.

Pettorelli, Nathalie, Jon Olav Vik, Atle Mysterud, Jean-Michel Gaillard, Compton J Tucker, and Nils Chr Stenseth. 2005. "Using the satellite-derived NDVI to assess ecological responses to environmental change." Trends in Ecology & Evolution 20 (9): 503–510.

Qin, Rongzhu, Zeyu Zhao, Jia Xu, Jian-Sheng Ye, Feng-Min Li, and Feng Zhang. 2022. "HRLT: a high-resolution (1 d, 1 km) and long-term (1961–2019) gridded dataset for surface temperature and precipitation across China." Earth System Science Data 14 (11): 4793–4810.

Train, Kenneth E., and Clifford Winston. "Vehicle choice behavior and the declining market share of US automakers." International economic review 48, no. 4 (2007): 1469-1496.

Tuholske, Cascade, Kelly Caylor, Chris Funk, Andrew Verdin, Stuart Sweeney, Kathryn Grace, Pete Peterson, and Tom Evans. "Global urban population exposure to extreme heat." Proceedings of the National Academy of Sciences 118, no. 41 (2021): e2024792118.

Wei, Jing, Zhanqing Li, Maureen Cribb et al. 2020. "Improved 1 km resolution PM2.5 estimates across China using enhanced space–time extremely randomized trees." Atmospheric Chemistry and Physics 20 (6): 3273–3289.

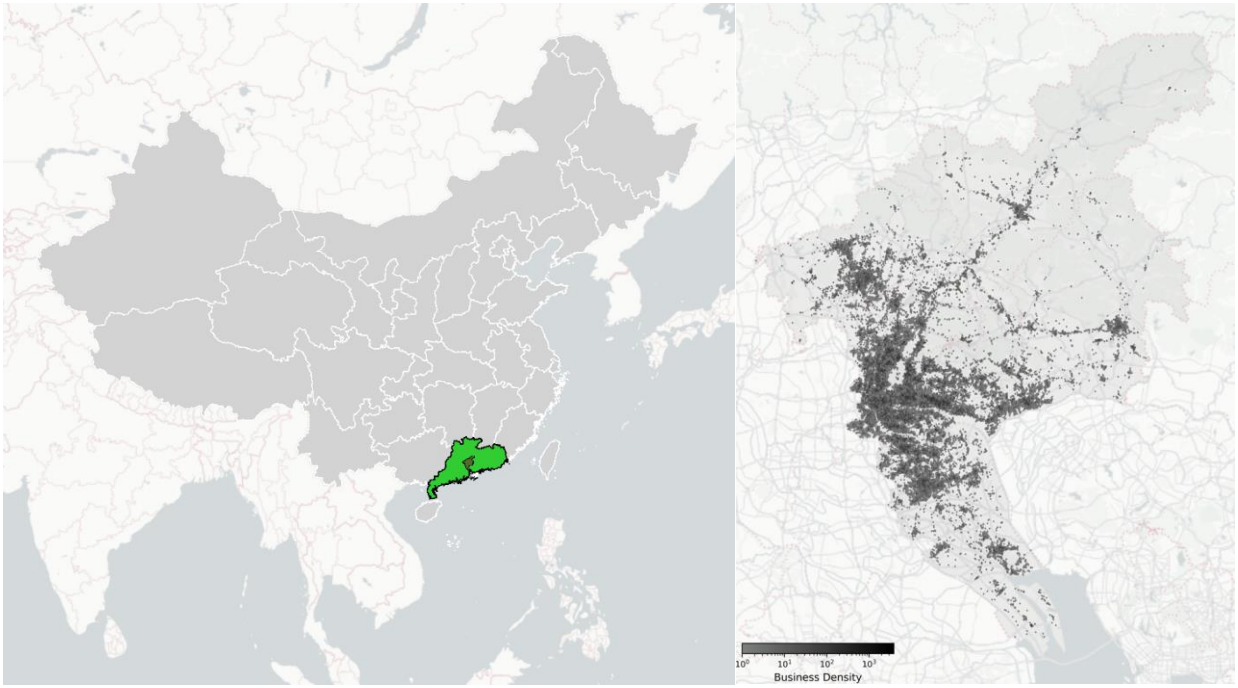
Wei, Jing, Zhanqing Li, Alexei Lyapustin, Lin Sun, Yiran Peng, Wenhao Xue, Tianning Su, and Maureen Cribb. 2021. "Reconstructing 1-km-resolution high-quality PM2. 5 data records from 2000 to 2018 in China: spatiotemporal variations and policy implications." Remote Sensing of Environment 252 112136.

Zhang, Tao, Yuyu Zhou, Zhengyuan Zhu, Xiaoma Li, and Ghassem R Asrar. 2021. "A globalseamless 1 km resolution daily land surface temperature dataset (2003–2020)." Earth System Science Data Discussions 2021 1–16.

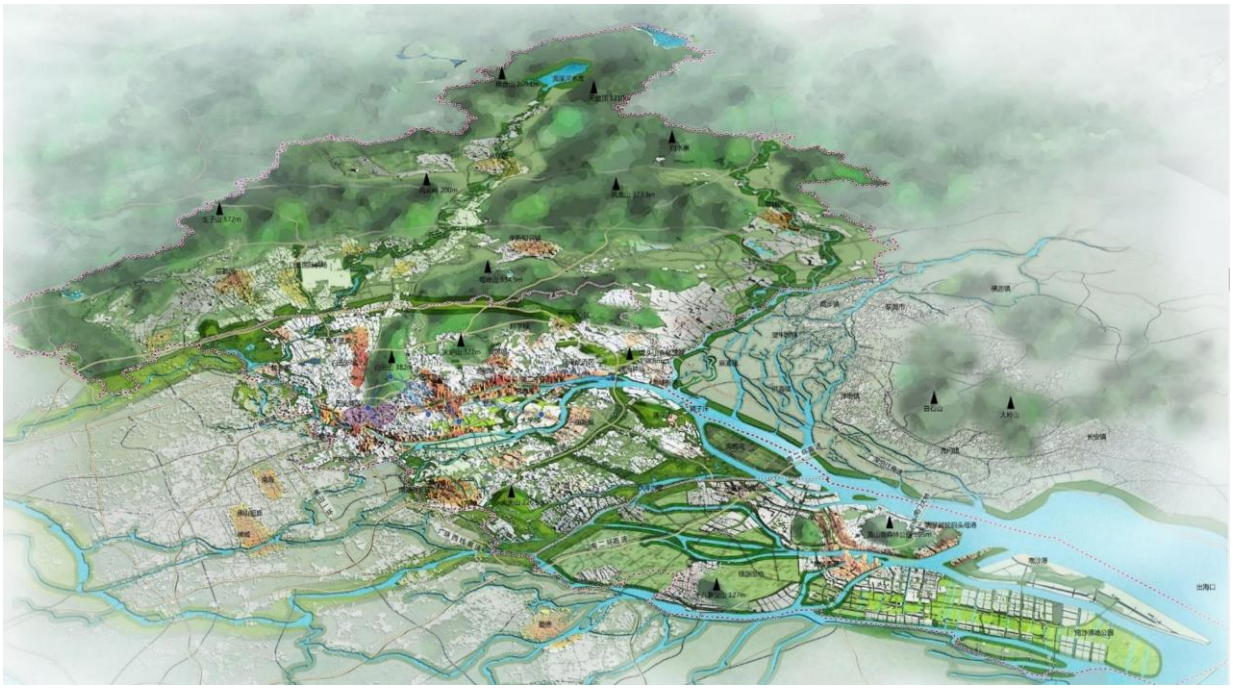
Figures and Tables

Figure 1. Economic and Ecological Layout

A. Guangzhou City and Business Distribution



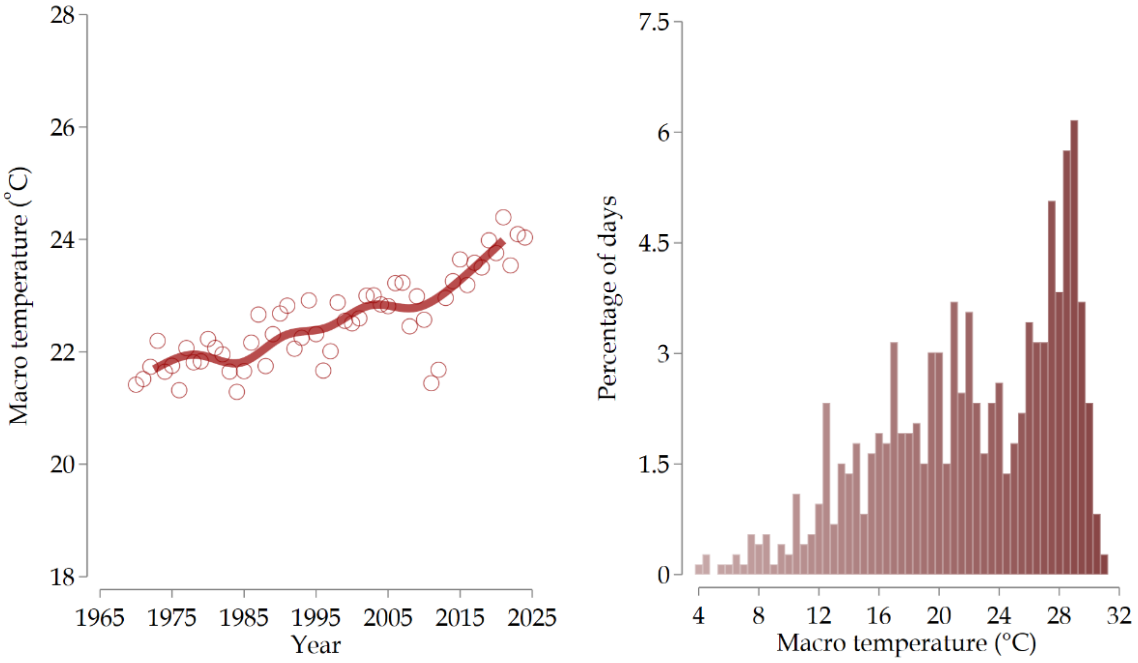
B. Aerial View of the City's Urban Ecology



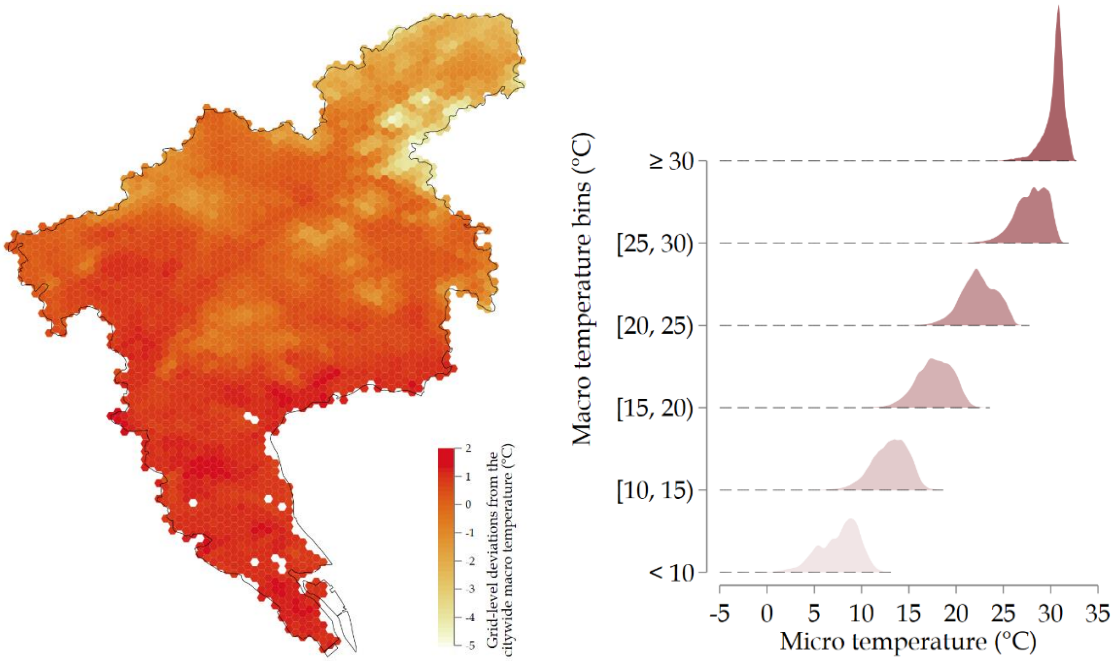
Notes: Panel A shows Guangzhou's location in southern China and maps the spatial footprint of restaurants and eateries used in our analysis. Panel B shows an aerial rendering of Guangzhou's landscape and ecological features, including mountainous terrain, river networks, and green infrastructure such as urban parks and tree-lined corridors.

Figure 2. Macro and Micro Temperature Patterns

A. Macro Temperature Trends and Distribution



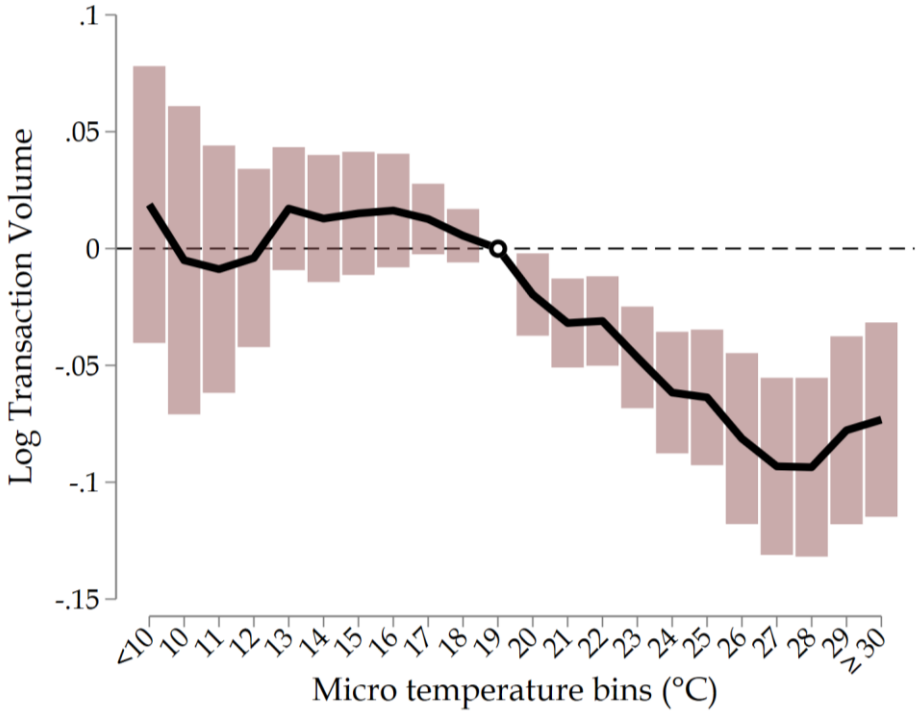
B. Micro Temperature Variability



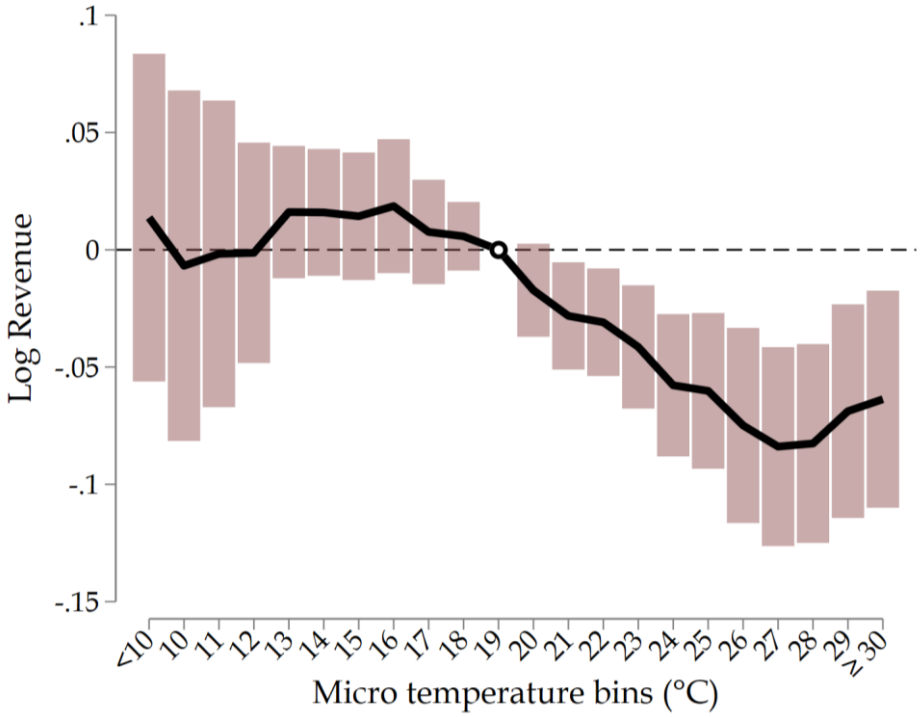
Notes: Panel A shows macro temperature trends and distributions. The left plot shows annual average daily temperatures from 1970 to 2024 overlaid with a median spline trendline. The right plot reports the distribution of citywide daily average temperatures during the 2018–2019 study period. Panel B left map plots 1 km hexagonal grid-level deviations from citywide daily averages. Blank spots correspond to water surfaces where temperature data are unavailable. The right plot shows the distribution of micro-level temperatures within each macro temperature bin.

Figure 3. Micro Temperature Shocks and Restaurant Business Outcomes

A. Transaction Volume

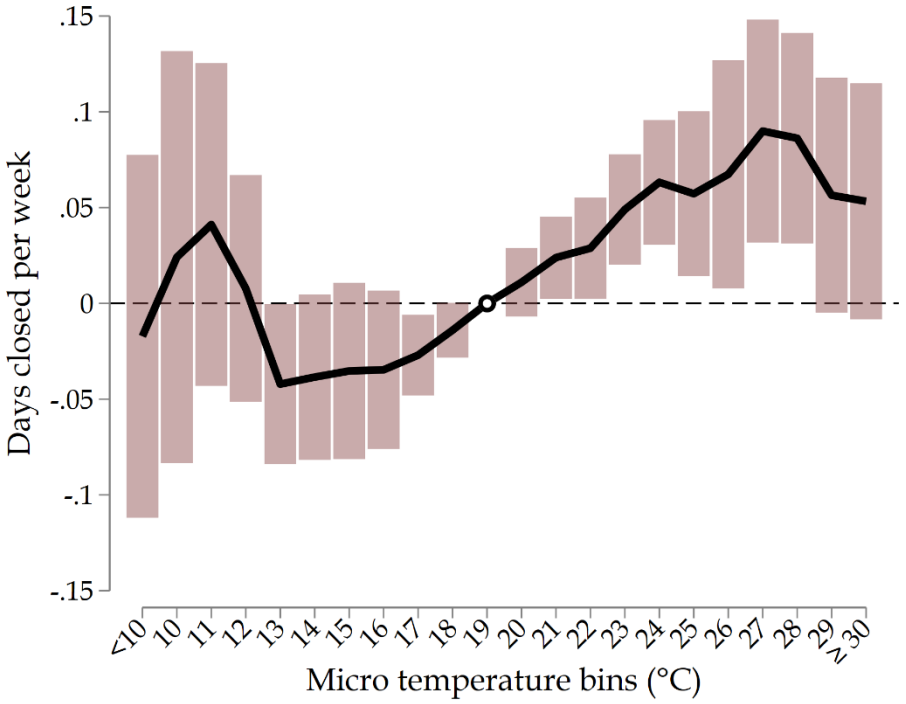


B. Revenue



Notes: The relationship between log of weekly transaction volume (Panel A) and weekly revenue (Panel B) against daily average micro temperature bins (in 1°C increment) surrounding each restaurant. The 19–20°C bin is the reference category. Regressions control for store fixed effects and week-of-sample fixed effects. Shaded bars show 95% confidence intervals based on standard errors clustered at the store and week levels.

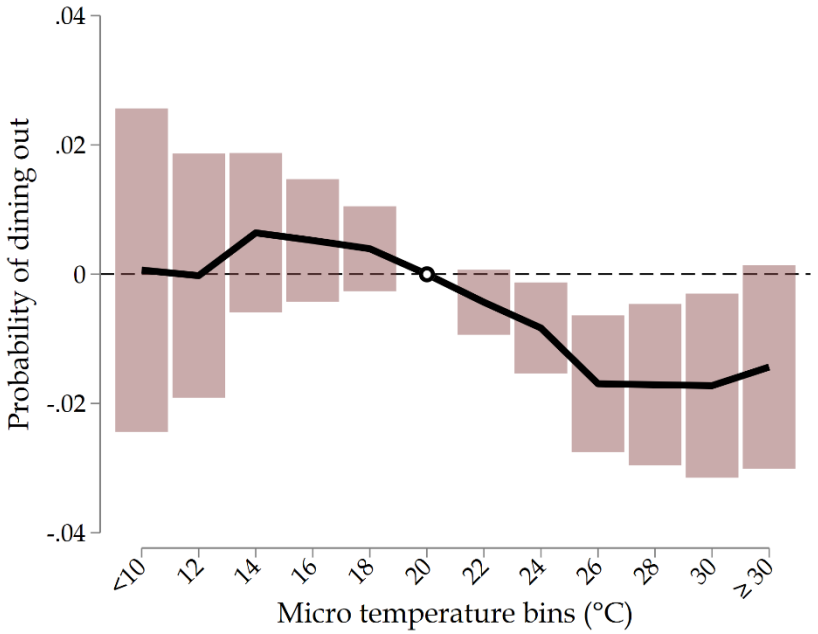
Figure 4. Merchant-Side Effect: Micro Temperature Shocks and Operation Status



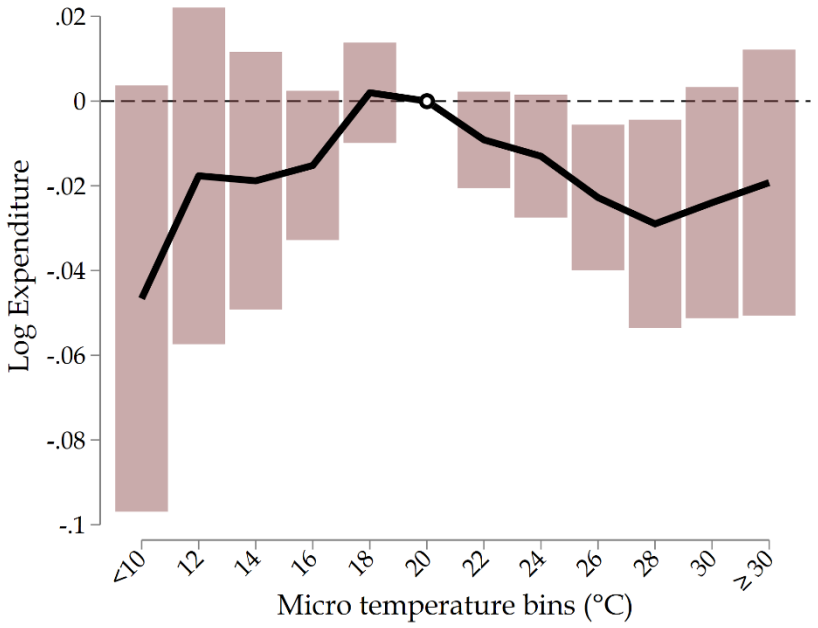
Notes: This figure plots the change in the number of days a restaurant is closed per week, as a function of microclimate temperature bins. The 19–20°C range is the reference category. Regression controls for store fixed effects and week-of-sample fixed effects. Shaded areas denote 95% confidence intervals, based on standard errors clustered at the store and week levels.

Figure 5. Consumer-Side Effect: Extensive vs Intensive Margins

A. Micro Temperature Shocks and Probability of Dining Out



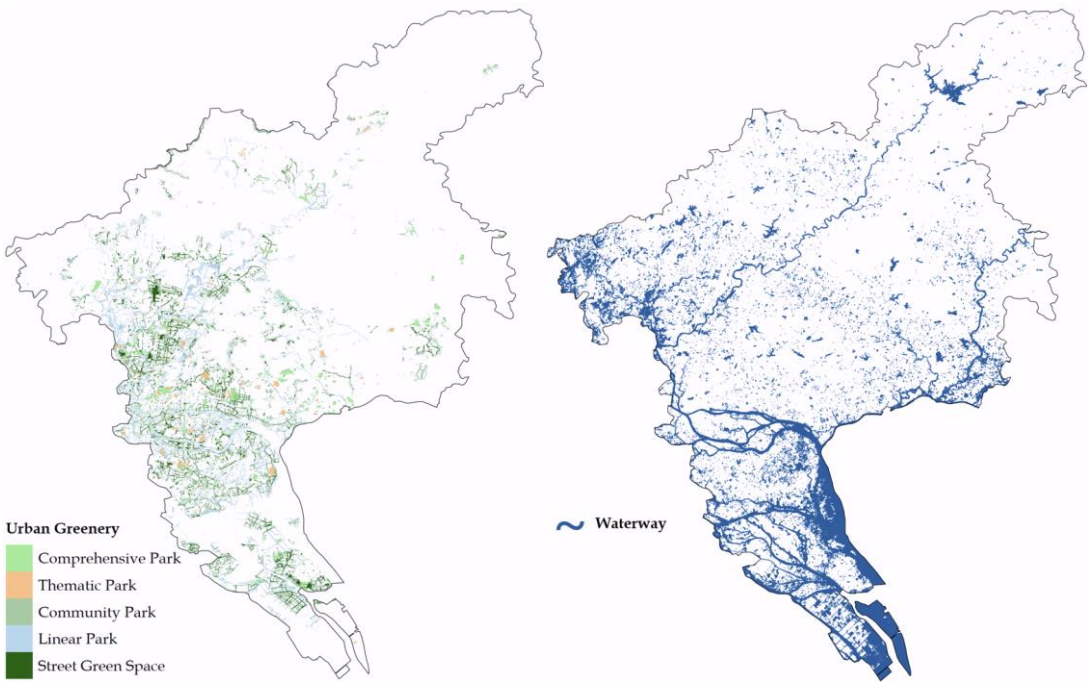
B. Micro Temperature Shocks and Expenditure



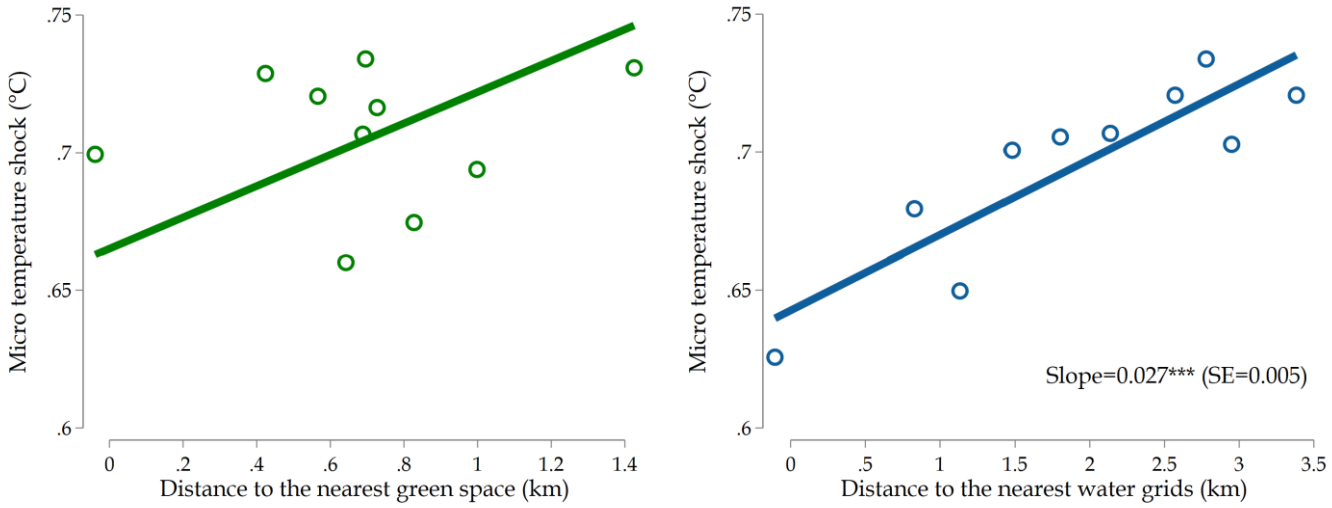
Notes: This figure shows changes in the weekly probability of dining out and the log of consumer expenditure, as a function of microclimate temperature bins (measured as the average temperature in lunch and dinner hub centers). The 18–20°C range is the reference category. Regression controls for consumer fixed effects and week-of-sample fixed effects. Shaded areas denote 95% confidence intervals, based on standard errors clustered at the consumer and week levels.

Figure 6. Urban Ecological Features and Micro Temperature

A. Distribution of Greenery and Waterways



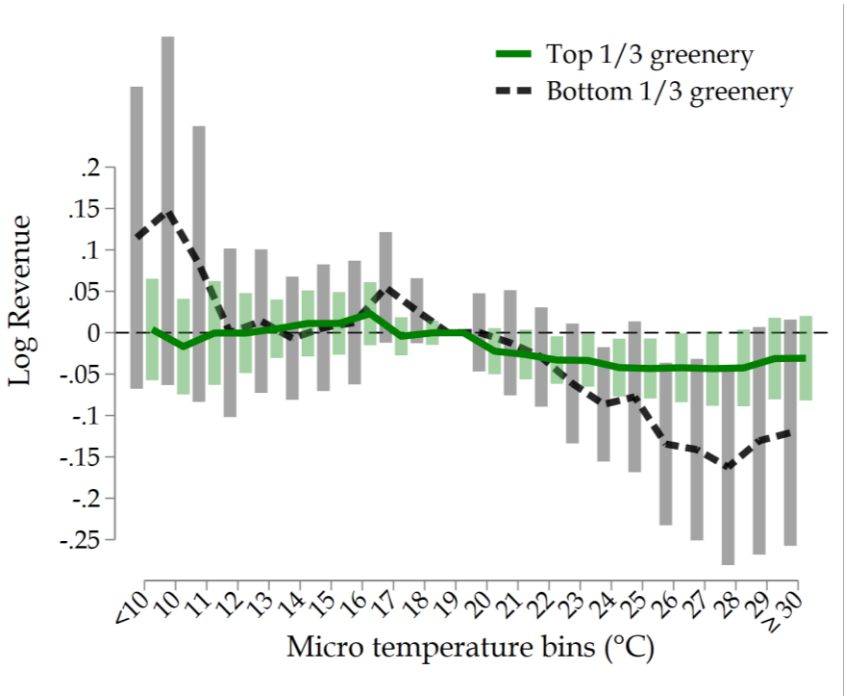
B. Relationships with Micro Temperature



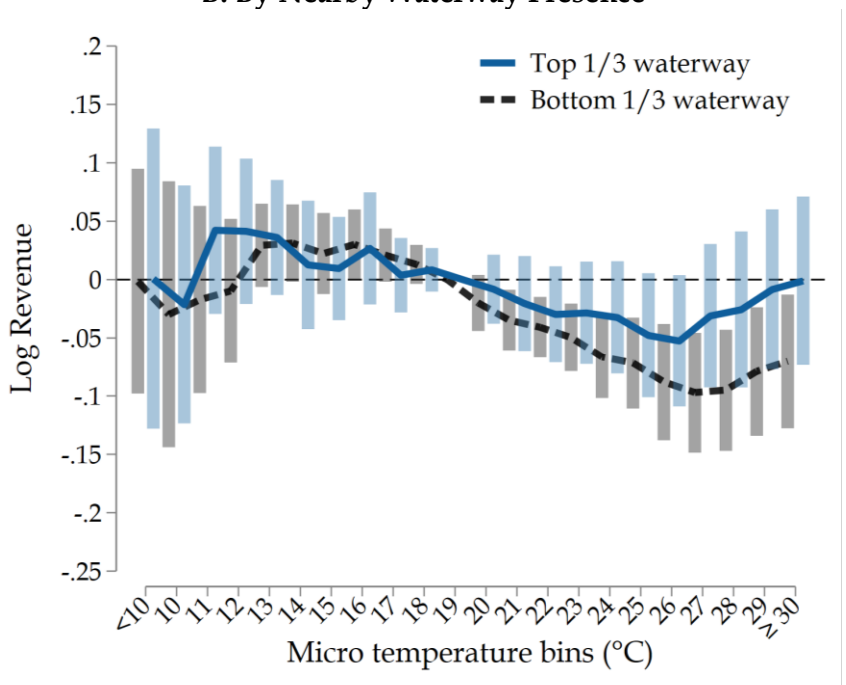
Notes: Panels A and B summarize the spatial distribution and mitigating effects of urban ecological features. In Panel A, the left map presents designated green spaces, while the right map shows water bodies identified via remote sensing. Panel B explores the relationship between microclimate temperature shocks and ecological proximity: the left graph plots a grid's average daily microclimate temperature deviation from the citywide macro temperature against its distance to the nearest green space, controlling for nearest-site fixed effects; the right graph presents the analogous relationship for proximity to the nearest waterway, controlling for nearest-waterway fixed effects. The analysis is limited to grids that contain at least one store.

Figure 7. Heterogeneity in Micro Temperature Responses

A. By Nearby Greenery Presence



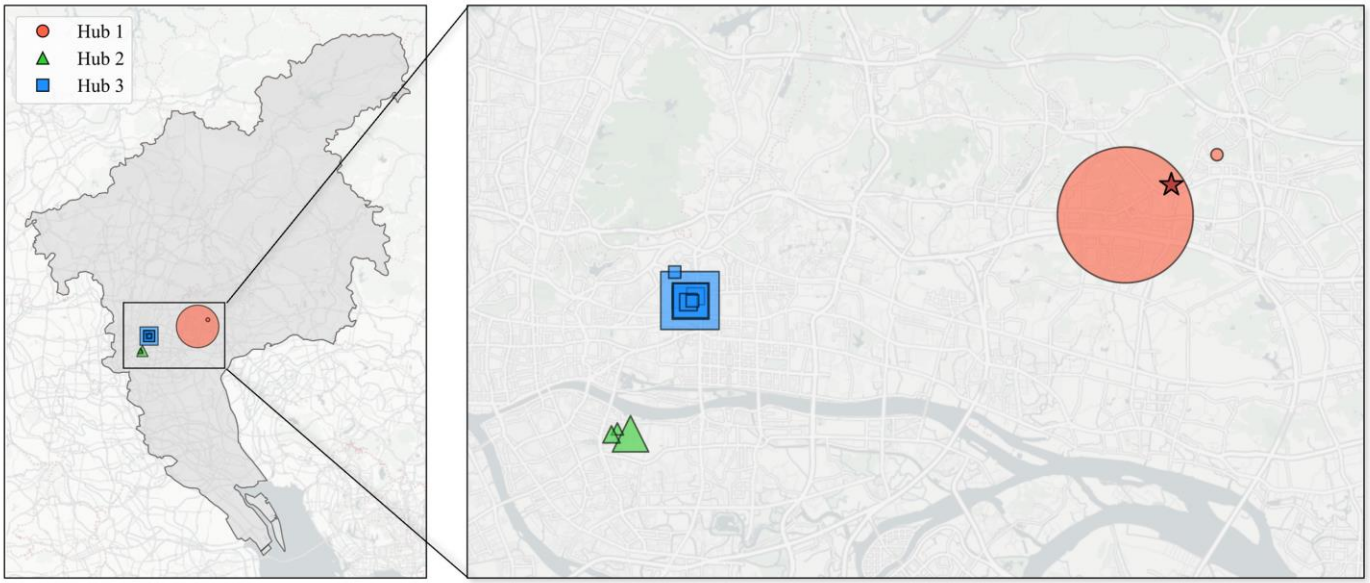
B. By Nearby Waterway Presence



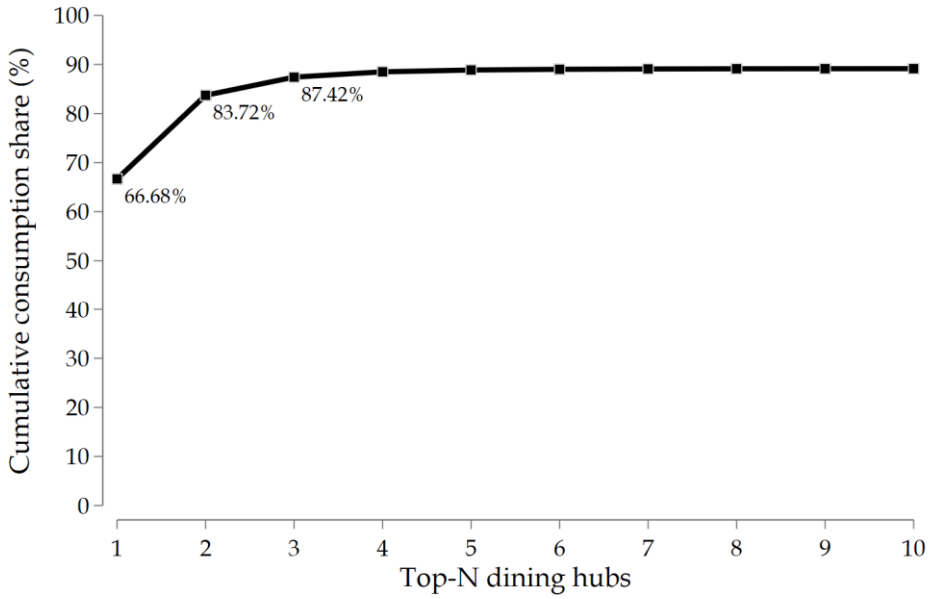
Notes: This figure shows heterogeneity in the relationship between micro temperature and restaurant revenue. Panel A compares restaurants located in areas with high versus low green space coverage (top versus bottom tercile). Panel B presents analogous results based on proximity to surface water. Regressions control for store and week fixed effects. Shaded bars denote 95% confidence intervals based on standard errors clustered at the store and week levels.

Figure 8. Consumer-Level Primary Dining Hub Identification

A. Clustering of Dining Choices for a Sample Consumer



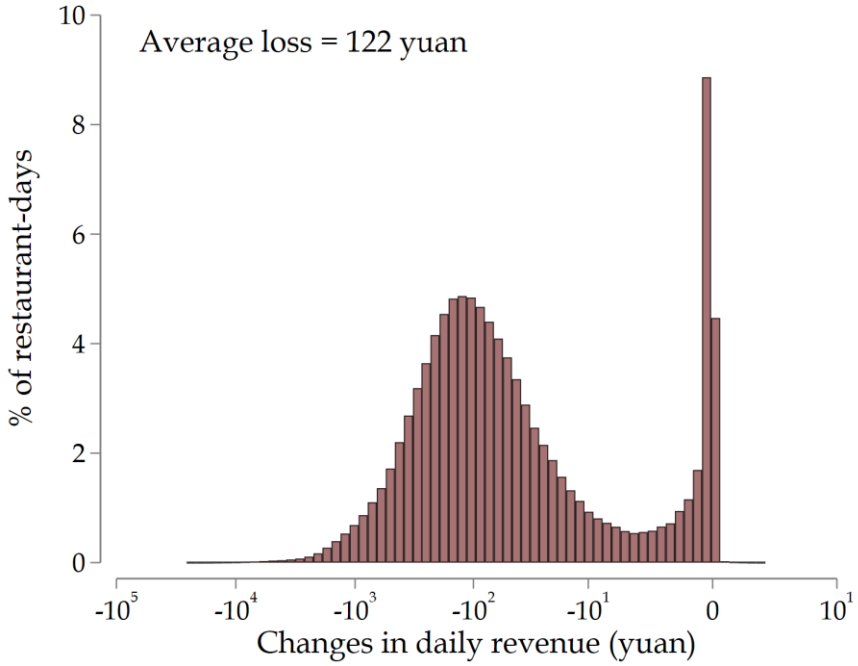
B. Cumulative Spending Across Top-N Dining Hubs (Full Sample)



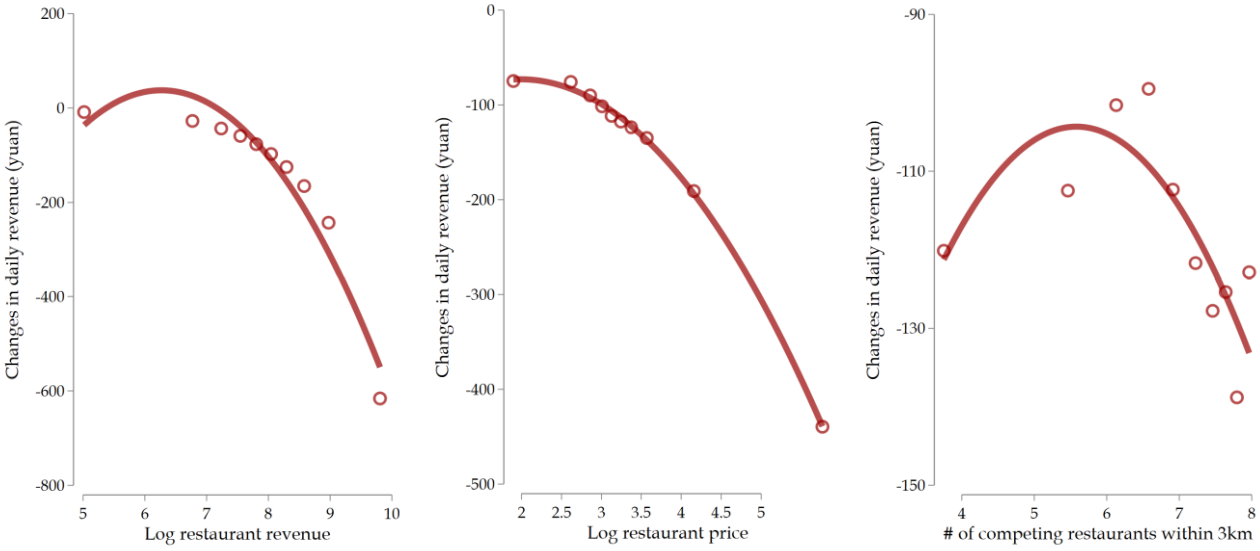
Notes: Panel A maps restaurant visits for an example consumer during weekday lunch hours. Each cluster of visits represents a dining hub, with the red star indicating the centroid of the primary (i.e., the largest) hub. Marker shapes and colors distinguish different clusters; marker sizes reflect visit frequency during the sample period. Panel B aggregates results across consumers, showing the cumulative share of spending accounted for by each consumer's top-N hubs. All clusters are detected using the HDBSCAN algorithm. Panel B reports the cumulative share of restaurant transactions accounted for by each individual's top-N dining hubs.

Figure 9. Counterfactual Analysis: Business Impacts of a 1°C Micro Temperature Warming

A. Distribution of Revenue Losses



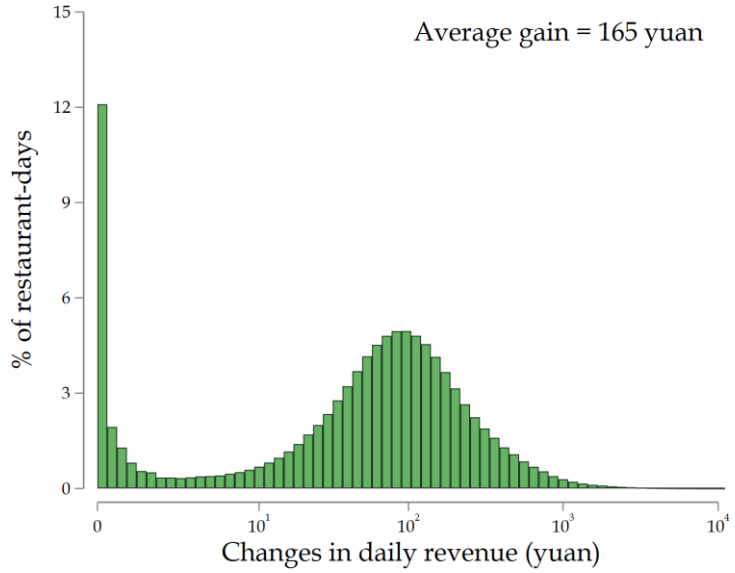
B. Heterogeneity by Store and Neighborhood Characteristics



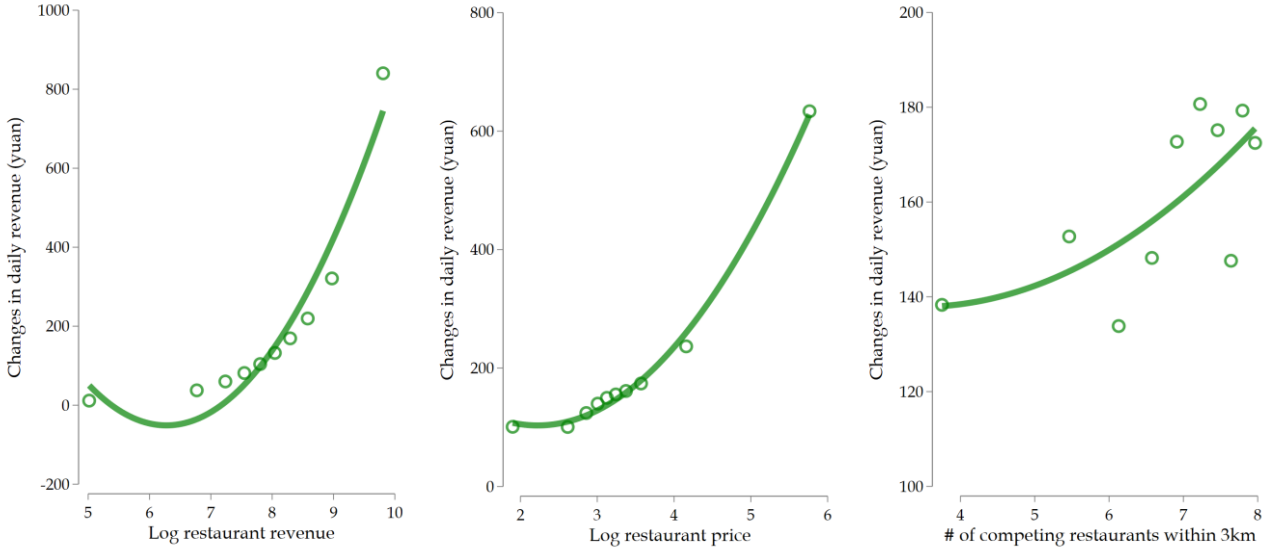
Notes: Panel A presents the distribution of daily revenue changes across restaurant-days under a 1°C increase in local micro temperature. Counterfactuals are simulated by perturbing each restaurant's local temperature while keeping all other spatial conditions fixed. Panel B explores heterogeneity in losses by restaurant characteristics (log revenue, pricing) and neighborhood context (density of nearby competitors within a 3 km radius).

Figure 10. Counterfactual Analysis: Business Value of Urban Green Space

A. Distribution of Revenue Gains



B. Heterogeneity by Store and Neighborhood Characteristics



Notes: Panel A presents the distribution of daily revenue changes across restaurant-days under a counterfactual scenario where each location's greenery share is raised from zero to its observed level. The average predicted revenue gain is 165 yuan per day. Panel B examines heterogeneity in these gains by store characteristics (log revenue, pricing) and neighborhood context (number of competing restaurants within a 3 km radius).

Table 1. Estimates of the Consumer Dining Choice Model

	[1]	[2]	[3]	[4]	[5]	[6]
Nonlinear Parameters						
Δ Day Temperature (℃)	-0.0146***			-0.0170***	-0.0146***	-0.0170***
	(0.0033)			(0.0033)	(0.0033)	(0.0033)
Δ Greenery share		0.0693***		0.0734***		0.0755***
		(0.0113)		(0.0114)		(0.0119)
Δ Waterway share			0.0727***		0.0345	-0.0178
			(0.0277)		(0.0289)	(0.0301)
Δ Pollution (mg/m³)	-0.0016	-0.0015	-0.0014	-0.0017*	-0.0016	-0.0017*
	(0.0010)	(0.0010)	(0.0010)	(0.0010)	(0.0010)	(0.0010)
Δ Precipitation (mm)	-0.0011	-0.0011	-0.0011	-0.0013	-0.0011	-0.0012
	(0.0015)	(0.0015)	(0.0015)	(0.0015)	(0.0015)	(0.0015)
Log(Distance)	-0.2987***	-0.2987***	-0.2987***	-0.2987***	-0.2987***	-0.2987***
	(0.0005)	(0.0005)	(0.0005)	(0.0005)	(0.0005)	(0.0005)
Observations	17,454,458	17,529,732	17,529,732	17,454,458	17,454,458	17,454,458
Linear Parameters						
Price (yuan)	-0.0196***	-0.0194***	-0.0194***	-0.0197***	-0.0196***	-0.0197***
	(0.0058)	(0.0058)	(0.0058)	(0.0058)	(0.0058)	(0.0058)
Restaurant FE	Yes	Yes	Yes	Yes	Yes	Yes
Date FE	Yes	Yes	Yes	Yes	Yes	Yes
Observations	3,098,342	3,098,342	3,098,342	3,098,342	3,098,342	3,098,342
Willingness to Pay (WTP)						
Temperature (*yuan*)	-0.745			-0.863	-0.745	-0.863
Greenery (*yuan*)		3.572		3.726		3.832
Waterway (*yuan*)			3.747		1.76	-0.904

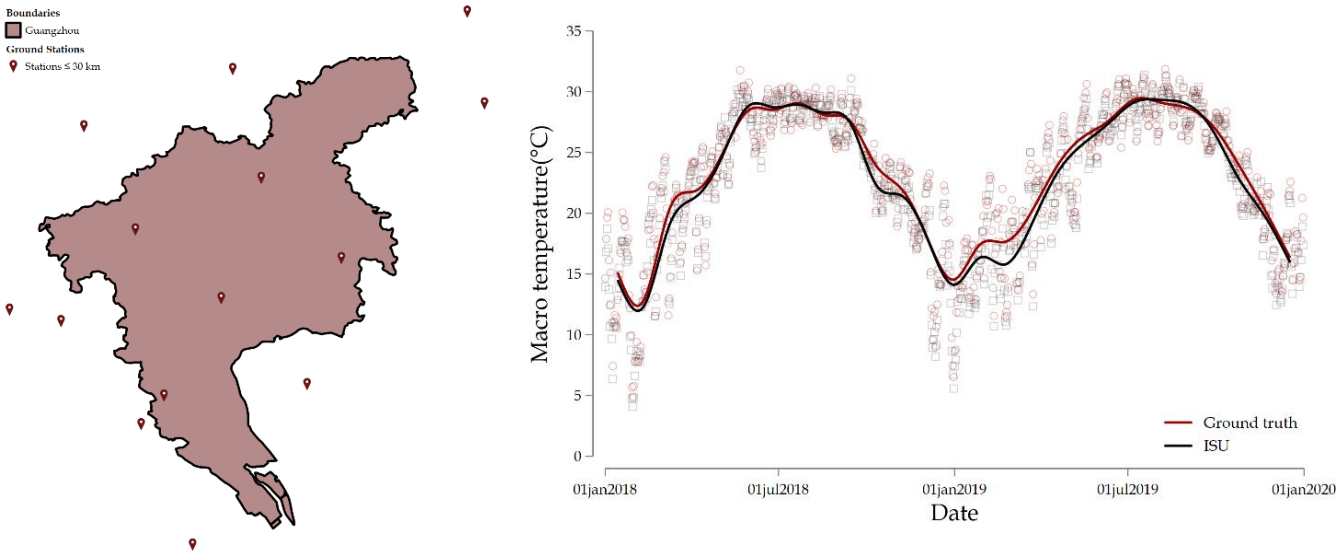
Notes: Δ represents the difference in environmental and ecological variables between stores and the centroid of the primary weekday lunch hub. Distance is defined as the length between stores and the centroid. The instrument used to estimate the price effect is the share of same-industry restaurants within a 3 km radius.

Table 2. Estimates of the Consumer Dining Choice Model Using On-route Temperature

	[1]	[2]	[3]	[4]
Nonlinear Parameters				
On-route Temperature (°C)	-0.0205**	-0.0308***	-0.0236***	-0.0312***
	(0.0088)	(0.0089)	(0.0088)	(0.0089)
Δ Greenery share		0.1717***		0.1413***
		(0.0156)		(0.0163)
Δ Waterway share			0.3124***	0.2228***
			(0.0335)	(0.0351)
Δ Pollution (mg/m³)	-0.0058***	-0.0061***	-0.0061***	-0.0063***
	(0.0013)	(0.0013)	(0.0013)	(0.0013)
Δ Precipitation (mm)	-0.0002	-0.0007	-0.0007	-0.0010
	(0.0021)	(0.0021)	(0.0021)	(0.0021)
Log(Distance)	-0.4194***	-0.4193***	-0.4194***	-0.4194***
	(0.0009)	(0.0009)	(0.0009)	(0.0009)
Observations	3,344,947	3,344,947	3,344,947	3,344,947
Linear Parameters				
Price (yuan)	-0.0139***	-0.0140***	-0.0139***	-0.0139***
	(0.0044)	(0.0045)	(0.0044)	(0.0045)
Restaurant FE	Yes	Yes	Yes	Yes
Date FE	Yes	Yes	Yes	Yes
Observations	1,362,146	1,362,146	1,362,146	1,362,146

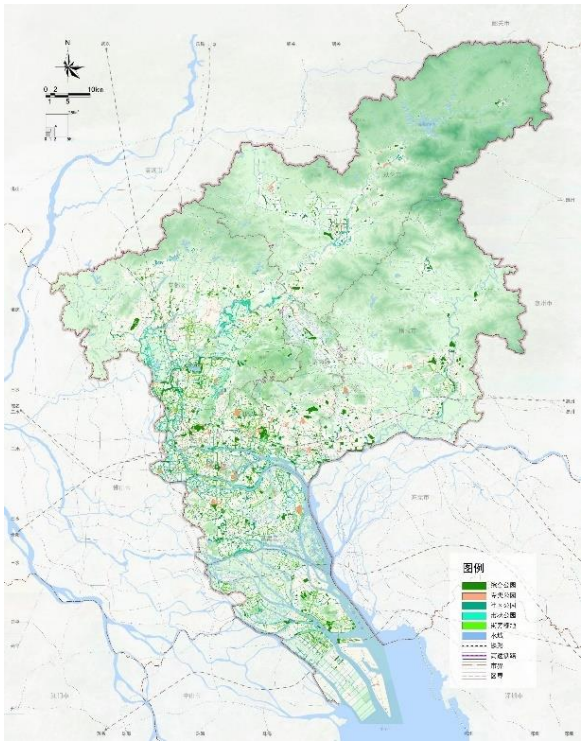
Appendix Figures and Tables

Appendix Figure 1. Remote-Sensing vs. Ground Truth Temperature Measures



Notes: The left panel maps the spatial distribution of 14 ground monitoring stations located within or up to 30 km from the Guangzhou city boundary. The right panel compares daily temperatures from ground stations (red dots) with those derived from the ISU remote-sensing dataset (black squares). Median splines (solid curves) are shown for both series.

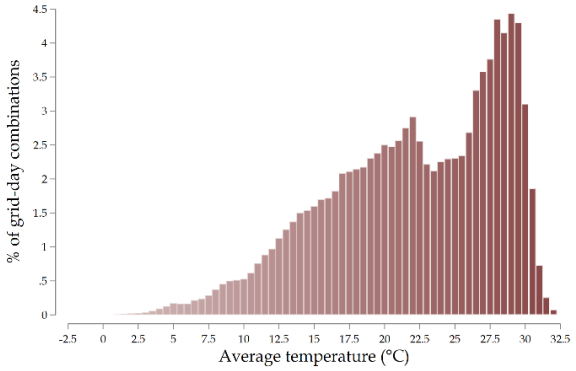
Appendix Figure 2. Distribution of Guangzhou's Green Space Constructions, 2010–2020



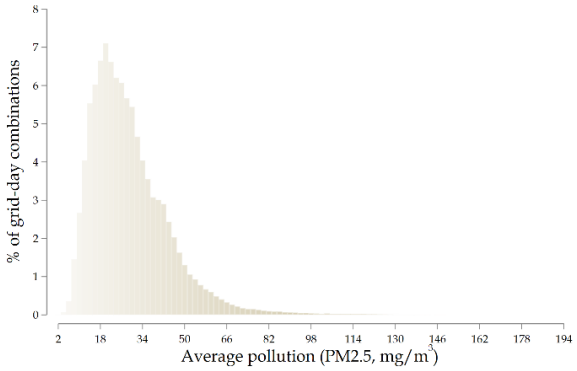
Notes: The original map of Guangzhou's Urban Green Space System for 2010–2020, including those for comprehensive parks, themed parks, community parks, pocket parks, buffer greenbelt, and water body.

Appendix Figure 3. Summary of Environmental Variables

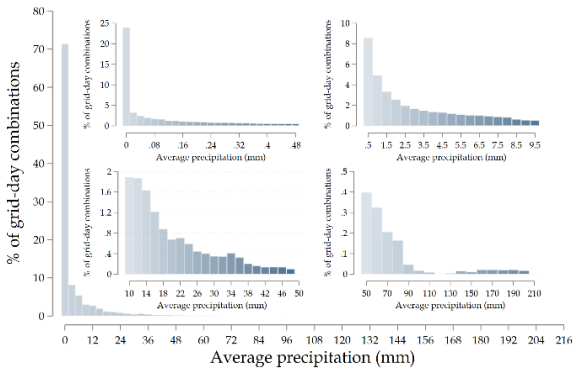
A. Temperature



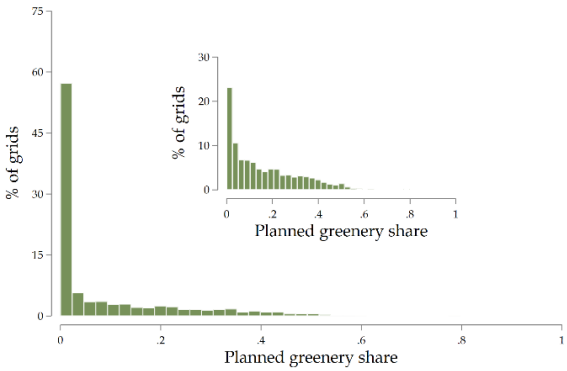
B. Pollution



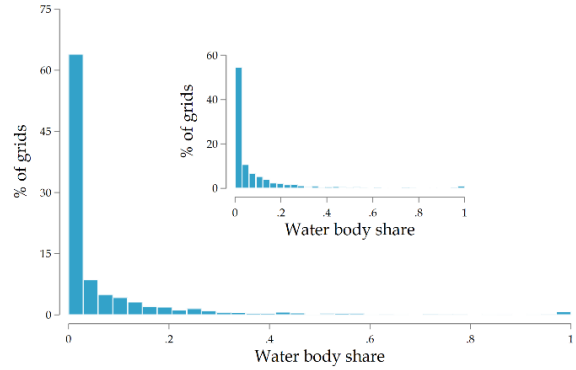
C. Precipitation



D. Greenery Share



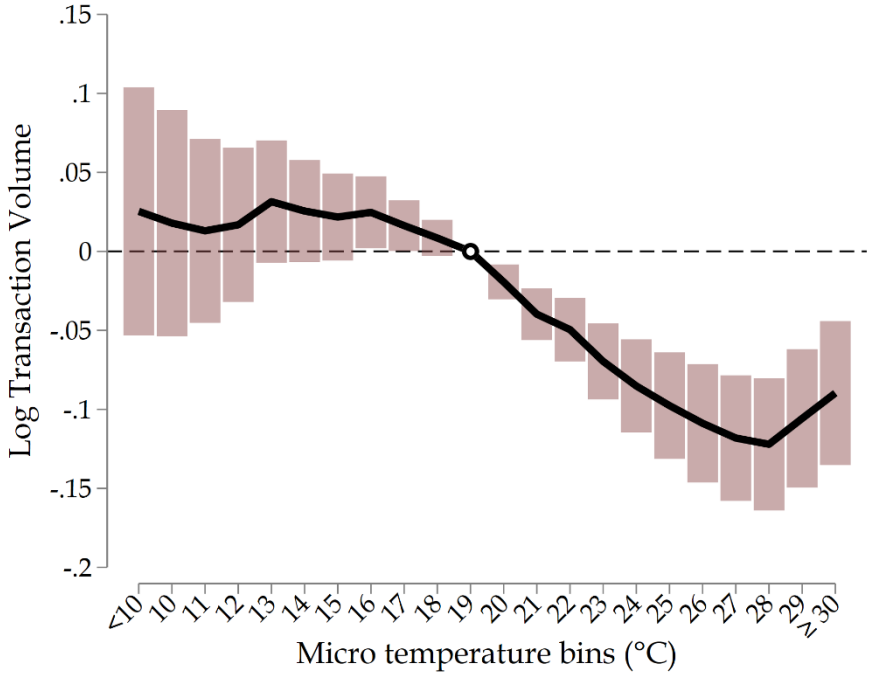
E. Water Body Share



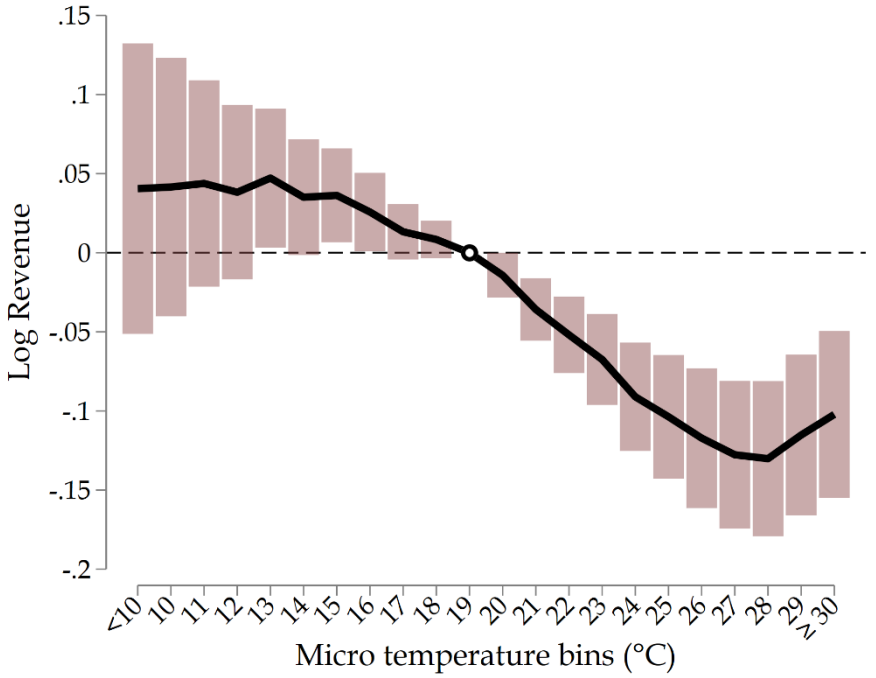
Notes: Panels A–C show the distributions of daily grid-level environmental conditions: temperature, PM2.5 pollution, and precipitation. Panels D and E illustrate the spatial distributions of planned green space and surface water coverage, respectively, across 1 km hexagonal grids. Inset plots provide zoomed-in views to highlight mass in the lower-value ranges. For precipitation, the four inset histograms correspond to average daily ranges of 0–0.5 mm, 0.5–10 mm, 10–50 mm, and >50 mm. For greenery and water body shares, inset views show distributions among grids with positive coverage.

Appendix Figure 4. Micro Temperature Shocks and Daily Business Outcomes

A. Transaction Volume



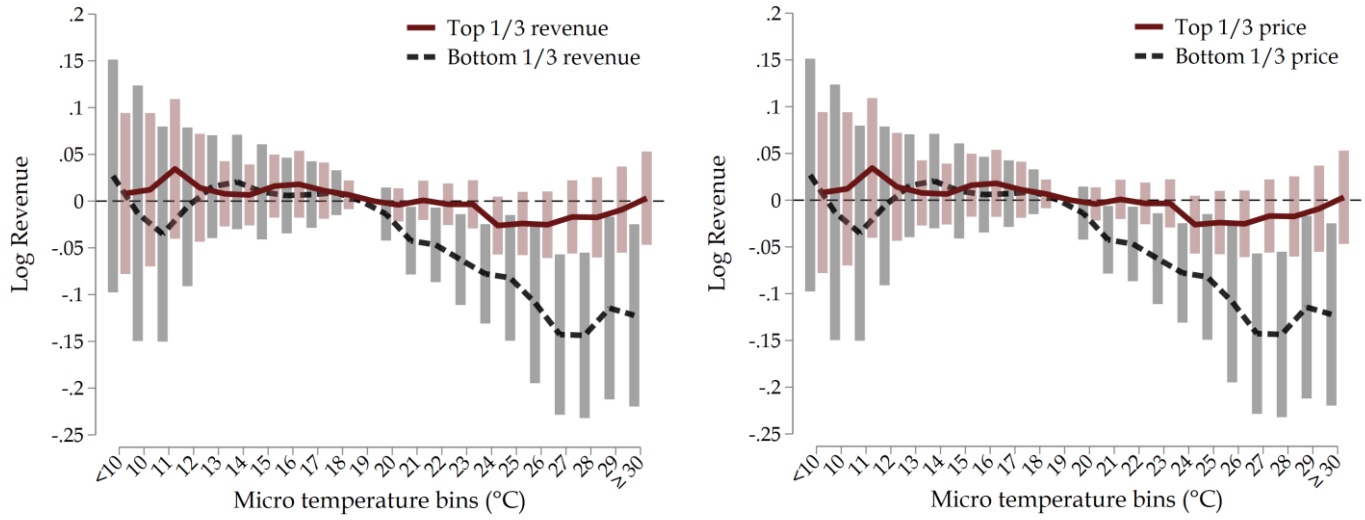
B. Revenue



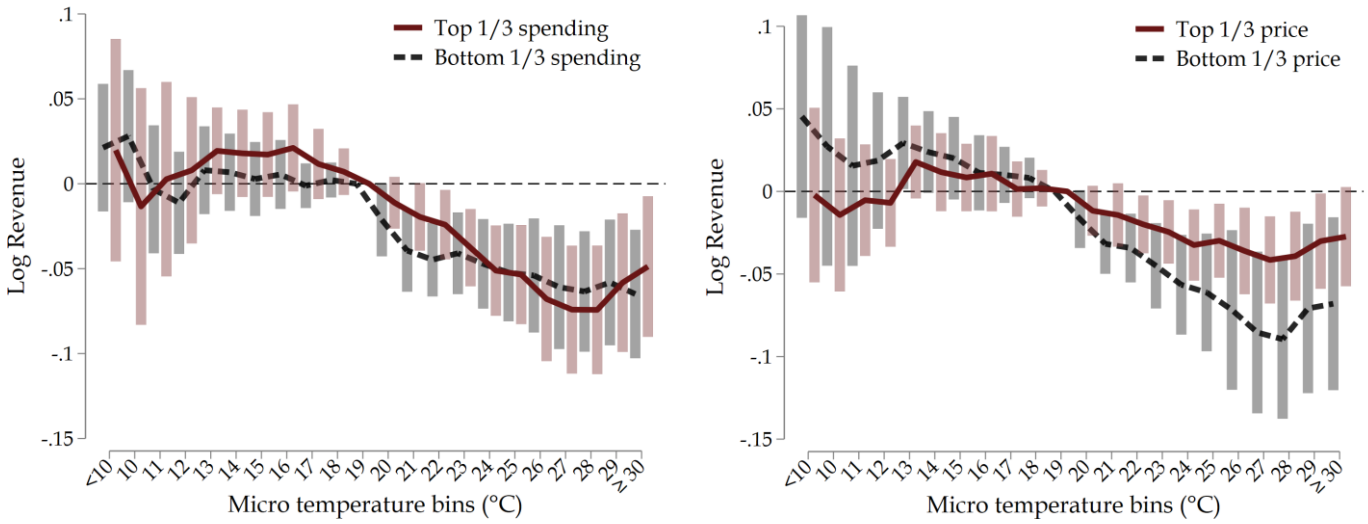
Notes: The relationship between log of weekly transaction volume (Panel A) and weekly revenue (Panel B) against daily average micro temperature bins (in 1°C increment) surrounding each restaurant. The 19–20°C bin is the reference category. Regressions control for store fixed effects and week-of-sample fixed effects. Shaded bars show 95% confidence intervals based on standard errors clustered at the store and week levels.

Appendix Figure 5. Heterogeneity in Micro Temperature Responses

A. By Merchant Characteristics



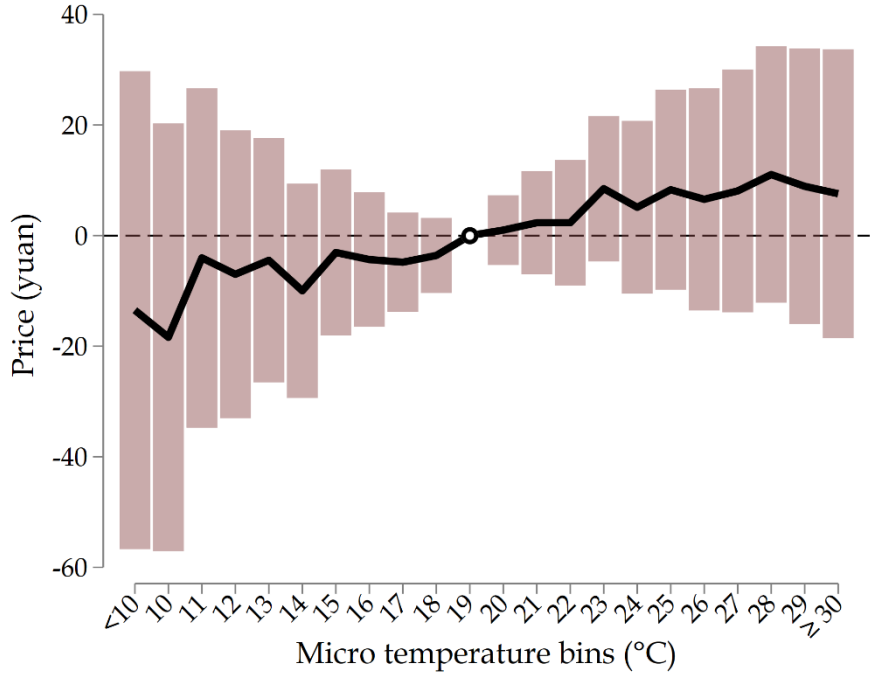
B. By Consumer Characteristics



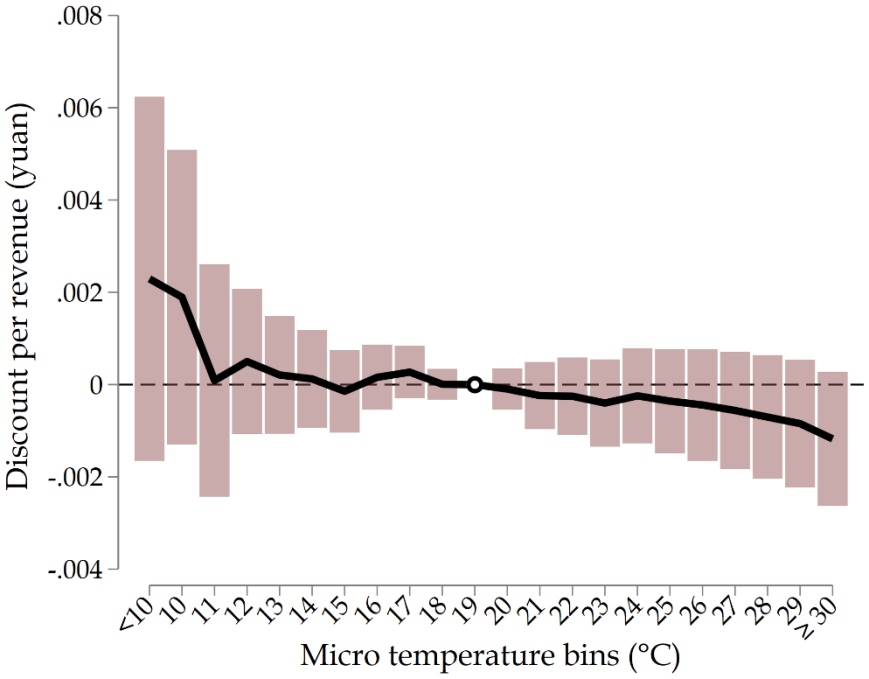
Notes: This figure shows heterogeneity in the relationship between micro temperature and restaurant revenue. Panel A estimates the effect of micro temperature shocks separately by merchant characteristics. The left panel compares merchants in the top versus bottom tercile of total revenue. The right panel compares merchants by price level (average revenue per transaction). Panel B presents analogous estimates by consumer characteristics. The left panel compares restaurant revenue generated by consumers in the top versus bottom tercile of total spending, and the right panel compares based on consumers' average spending per transaction. Regressions include store fixed effects and week-of-sample fixed effects. Shaded bars indicate 95% confidence intervals based on standard errors clustered at the store and week levels.

Appendix Figure 6. Merchant-Side Effect: Price and Discount

A. Price



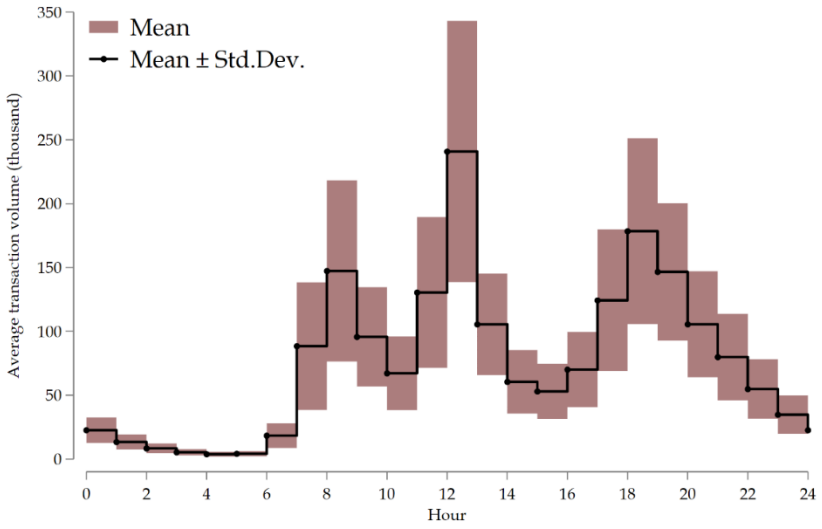
B. Discount



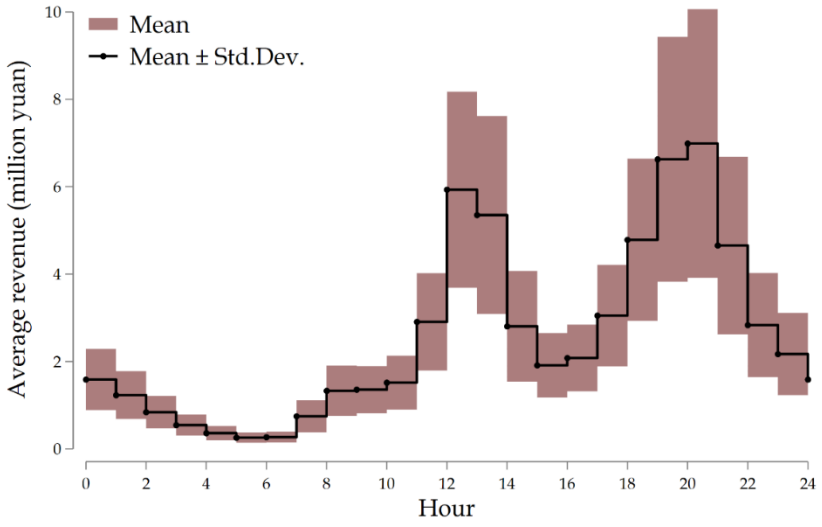
Notes: The relationship between price (Panel A) and discount per revenue (Panel B) against daily average micro temperature bins (in 1°C increment) surrounding each restaurant. The 19–20°C bin is the reference category. Regressions control for store fixed effects and week-of-sample fixed effects. Shaded bars show 95% confidence intervals based on standard errors clustered at the store and week levels

Appendix Figure 7. Distribution of Restaurant Business Hours

A. Transaction Volume



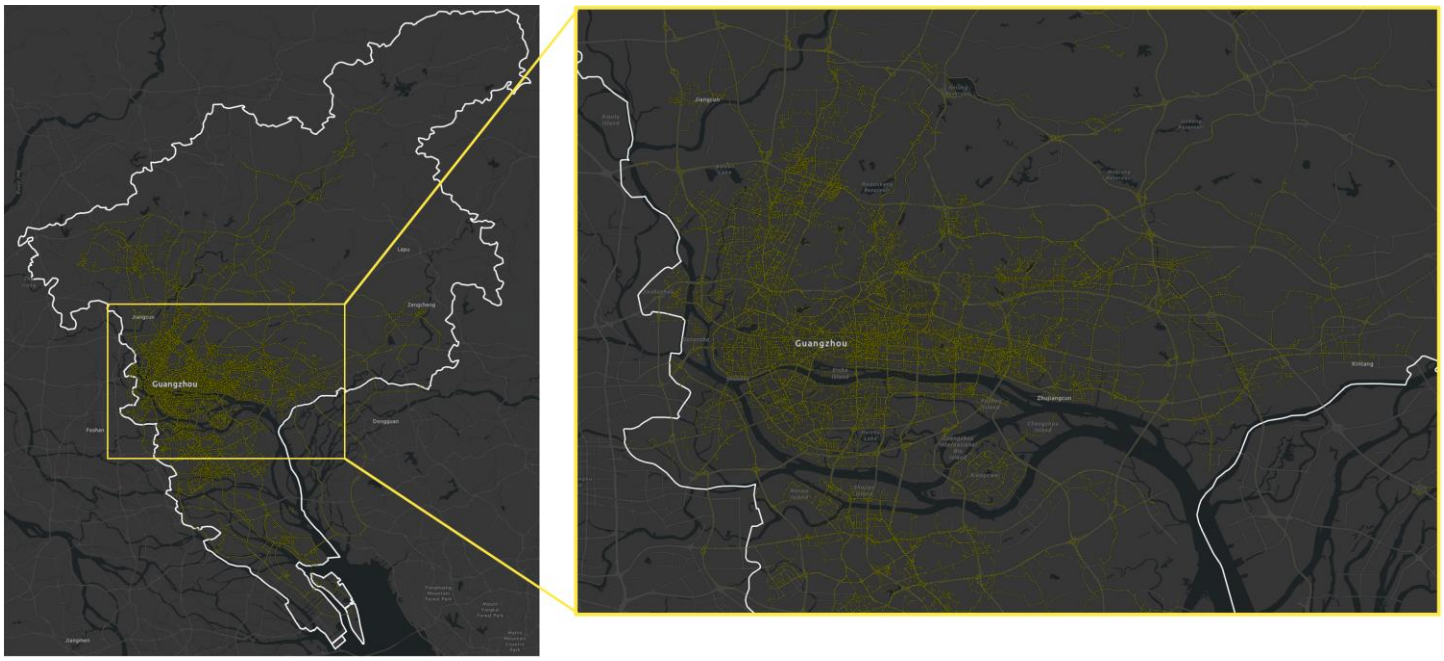
B. Revenue



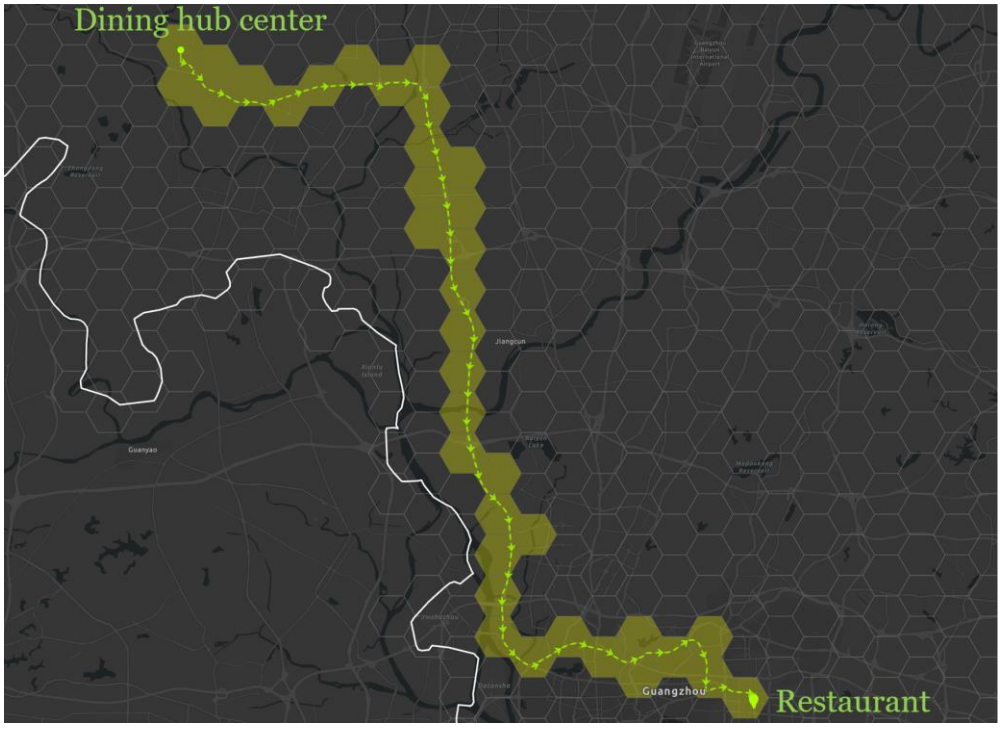
Notes: Panel A plots the average hourly transaction volume across restaurants, while Panel B shows corresponding hourly revenue. Shaded bars represent means with bands denoting one standard deviation above and below. The two peaks in both transaction count and revenue correspond to typical midday and evening dining periods. Based on these patterns, we define lunch hours as 11:00–14:00 and dinner hours as 17:00–22:00 for the analysis.

Appendix Figure 8. Measurement of On-route Temperature

A. Distribution of Shortest Travel Time Routes



B. Illustrative Example



Notes: Panel A displays the shortest-time routes between each dining hub center and sampled restaurants, which align precisely with the road network data. Panel B presents an example illustrating how on-route temperature is measured—as the average temperature of all hexagonal grids traversed along the efficient route from the dining hub center to the restaurant.

Appendix Table 1. Summary Statistics

	Obs	Mean	SD	Min	P25	P50	P75	Max
Panel A: Environment Data (Hexagonal grid-daily)								
Ave Temp	1921360	22.34	6.14	-2.05	17.98	23.02	27.77	32.67
Mid-day Temp	1921360	26.02	6.45	-1.60	21.70	26.90	31.40	38.30
Mid-night Temp	1921360	18.66	6.12	-4.20	14.07	19.50	24.30	28.90
PM2.5 *($\mu g/m^3$)*	1936690	30.03	15.02	2.35	19.45	27.05	37.30	186.65
Precipitation (*mm*)	1938150	4.86	12.13	0.00	0.03	0.50	4.16	213.12
%Planned Greenery	2061520	0.09	0.14	0.00	0.00	0.00	0.13	0.80
%Water Body	2061520	0.08	0.16	0.00	0.00	0.01	0.07	1.00
Panel B: Economic Data (Restaurant-weekly)								
Consumer Traffic	2040445	648.38	1304.86	0.00	26.00	233.00	768.00	129355.00
Revenue (*1000 yuan*)	2040445	21.75	48.46	0.00	2.22	8.88	22.74	3765.86
Per-trans Value (*yuan*)	2038980	302.25	1489.38	0.01	14.02	23.07	149.90	301049.69
#Weekly Closed Days	2038980	1.39	2.16	0.00	0.00	0.00	3.00	6.00

Notes: This table reports summary statistics for the main environmental and economic variables used in the analysis. Panel A presents grid-day level environmental data, including average, mid-day, and mid-night land surface temperatures (°C), air pollution measured by PM2.5 concentration ($\mu g/m^3$), precipitation (mm), and the share of each hexagonal grid covered by planned green space or water bodies. Panel B summarizes restaurant-week level economic data, including weekly consumer traffic, total revenue (in thousands of yuan), average value per transaction (yuan), and the number of days closed per week.

Appendix Table 2. Estimates of the Consumer Dining Choice Model (Dinner)

	[1]	[2]	[3]	[4]	[5]	[6]
Nonlinear Parameters						
Δ Night Temperature (℃)	-0.0466***			-0.0538***	-0.0470***	-0.0530***
	(0.0090)			(0.0090)	(0.0090)	(0.0090)
Δ Greenery share		0.1635***		0.1667***		0.1761***
		(0.0108)		(0.0108)		(0.0112)
Δ Waterway share			0.0110		0.0313	-0.0928***
			(0.0291)		(0.0300)	(0.0310)
Δ Pollution (mg/m³)	0.0015	0.0011	0.0014	0.0013	0.0015	0.0014
	(0.0010)	(0.0010)	(0.0010)	(0.0010)	(0.0010)	(0.0010)
Δ Precipitation (mm)	-0.0002	-0.0006	-0.0001	-0.0006	-0.0002	-0.0006
	(0.0015)	(0.0014)	(0.0014)	(0.0015)	(0.0015)	(0.0015)
Log(Distance)	-0.3301***	-0.3293***	-0.3295***	-0.3298***	-0.3301***	-0.3298***
	(0.0005)	(0.0005)	(0.0005)	(0.0005)	(0.0005)	(0.0005)
Observations	33,205,101	33,397,240	33,397,240	33,205,101	33,205,101	33,205,101
Linear Parameters						
Price (yuan)	-0.0160***	-0.0162***	-0.0161***	-0.0161***	-0.0160***	-0.0161***
	(0.0048)	(0.0048)	(0.0048)	(0.0048)	(0.0048)	(0.0048)
Restaurant FE	Yes	Yes	Yes	Yes	Yes	Yes
Date FE	Yes	Yes	Yes	Yes	Yes	Yes
Observations	6,472,595	6,503,798	6,503,798	6,472,595	6,472,595	6,472,595
Willingness to Pay (WTP)						
Temperature (*yuan*)	-2.913			-3.342	-2.938	-3.292
Greenery (*yuan*)		10.093		10.354		10.938
Waterway (*yuan*)			0.683		1.956	-5.764

Notes: Δ represents the difference in environmental and ecological variables between stores and the centroid of the primary dinner hub. Distance is defined as the length between stores and the centroid. The instrument used to estimate the price effect is the share of same-industry restaurants within a 3 km radius.

Appendix Table 3. Estimates of the Consumer Dining Choice Model with Interaction Terms

	[1]	[2]	[3]	[4]
Nonlinear Parameters				
Δ Day Temperature (°C)	-0.0205***	-0.0163***	-0.0145***	-0.0160***
	(0.0033)	(0.0033)	(0.0033)	(0.0033)
Δ NDVI	-0.3214***			
	(0.0168)			
Δ Greenery share		0.0746***		0.0773***
		(0.0114)		(0.0118)
Δ Waterway share			0.0339	-0.0202
			(0.0288)	(0.0300)
Δ Day Temperature (°C) × Δ Greenery share		0.0988***		0.1202***
		(0.0149)		(0.0154)
Δ Day Temperature (°C) × Δ Waterway share			-0.1224***	-0.1988***
			(0.0346)	(0.0355)
Δ Pollution (mg/m^3)	-0.0027***	-0.0017*	-0.0016	-0.0017*
	(0.0010)	(0.0010)	(0.0010)	(0.0010)
Δ Precipitation (mm)	-0.0015	-0.0013	-0.0011	-0.0013
	(0.0015)	(0.0015)	(0.0015)	(0.0015)
Log(Distance)	-0.2994***	-0.2990***	-0.2987***	-0.2990***
	(0.0005)	(0.0005)	(0.0005)	(0.0005)
Observations	17,454,458	17,454,458	17,454,458	17,454,458
Linear Parameters				
Price (yuan)	-0.0196***	-0.0197***	-0.0196***	-0.0198***
	(0.0058)	(0.0059)	(0.0058)	(0.0059)
Restaurant FE	Yes	Yes	Yes	Yes
Date FE	Yes	Yes	Yes	Yes
Observations	3,098,342	3,098,342	3,098,342	3,098,342

Notes: Δ represents the difference in environmental and ecological variables between stores and the centroid of the primary weekday lunch hub. Distance is defined as the length between stores and the centroid. The instrument used to estimate the price effect is the share of same-industry restaurants within a 3 km radius.

Appendix Table 4. Transportation and Consumer Adaptation

	[1]
Nonlinear Parameters	
Δ Temperature (℃)	-0.051977***
	(0.004829)
Δ Temperature (℃) × Distance to the Nearest Bus Station	0.169605***
	(0.016085)
Δ Pollution (mg/m³)	-0.001380
	(0.001077)
Δ Precipitation (mm)	-0.000940
	(0.001541)
Log(Distance)	-0.296534***
	(0.000465)
Observations	16,754,899
Linear Parameters	
Price (yuan)	-0.0175***
	(0.0054)
Restaurant FE	Yes
Date FE	Yes
Observations	2,608,586

Notes: Δ represents the difference in environmental and ecological variables between stores and the centroid of the primary weekday lunch hub. Distance is defined as the length between stores and the centroid. The instrument used to estimate the price effect is the share of same-industry restaurants within a 3 km radius.

Appendix Table 5. Commercial Space Rental Price and Microclimate Temperature

	[1]	[2]	[3]
Mean micro temperature shock (std.)	-0.038	-0.019	-0.016
	(0.0090)	(0.0006)	(0.0108)
District FE	No	Yes	Yes
Property Characteristics	No	No	Yes
Observations	29,750	29,750	29,750

Notes: Mean micro temperature shocks are defined as average grid-level deviations from the citywide macro temperature. Rental data were collected for Guangzhou from September 2023 to June 2024 via 58.com. "Property characteristics" include fixed effects dummies for operation status (vacant, operating), business sector (e.g., food, beverage), location type (e.g., street-facing storefront, in-mall units), and floor. Standard errors are clustered at the district level.